JOURNAL OF VIROLOGY, Feb. 2006, p. 1497–1512 Vol. 80, No. 3
0022-538X/06/$08.00+0 doi:10.1128/JVI.80.3.1497–1512.2006

The Cellular Localization Pattern of Varicella-Zoster Virus ORF29p Is Influenced by Proteasome-Mediated Degradation

Christina L. Stallings,[1,2] Gregory J. Duigou,[2] Anne A. Gershon,[3] Michael D. Gershon,[4] and Saul J. Silverstein[1,2]*

Integrated Program in Cellular, Molecular and Biophysical Studies[1] and Departments of Microbiology,[2] Pediatrics,[3] and Pathology and Cell Biology,[4] Columbia University, College of Physicians and Surgeons, 701 W. 168th St., New York, New York 10032

Received 22 June 2005/Accepted 11 November 2005

Varicella-zoster virus (VZV) open reading frame 29 (ORF29) encodes a single-stranded DNA binding protein. During lytic infection, ORF29p is localized primarily to infected-cell nuclei, whereas during latency it appears in the cytoplasm of infected neurons. Following reactivation, ORF29p accumulates in the nucleus. In this report, we analyze the cellular localization patterns of ORF29p during VZV infection and during autonomous expression. Our results demonstrate that ORF29p is excluded from the nucleus in a cell-type-specific manner and that its cellular localization pattern may be altered by subsequent expression of VZV ORF61p or herpes simplex virus type 1 ICP0. In these cases, ORF61p and ICP0 induce nuclear accumulation of ORF29p in cell lines where it normally remains cytoplasmic. One cellular system utilized by ICP0 to influence protein abundance is the proteasome degradation pathway. Inhibition of the 26S proteasome, but not heat shock treatment, resulted in accumulation of ORF29p in the nucleus, similar to the effect of ICP0 expression. Immunofluorescence microscopy and pulse-chase experiments reveal that stabilization of ORF29p correlates with its nuclear accumulation and is dependent on a functional nuclear localization signal. ORF29p nuclear translocation in cultured enteric neurons and cells derived from an astrocytoma is reversible, as the protein's distribution and stability revert to the previous states when the proteasomal activity is restored. Thus, stabilization of ORF29p leads to its nuclear accumulation. Although proteasome inhibition induces ORF29p nuclear accumulation, this is not sufficient to reactivate latent VZV or target the immediate-early protein ORF62p to the nucleus in cultured guinea pig enteric neurons.

Chicken pox (varicella) is a manifestation of lytic infection of cutaneous epithelial cells by varicella-zoster virus (VZV), a ubiquitous human alphaherpesvirus. Following lytic infection, VZV establishes latency in the sensory ganglia and can reactivate later during the host's life to cause shingles (zoster), a painful and potentially debilitating disease that may lead to postherpetic neuralgia (1). Recrudescence occurs when cell-mediated immunity is decreased, as seen in the elderly and immunocompromised individuals, where it is associated with significant morbidity that may not be relieved by antiviral and analgesic therapy (63). An understanding of the cellular and viral factors that govern VZV latency and reactivation is critical to developing preventive methods and potential therapies for zoster and postherpetic neuralgia.

During latency, viral DNA replication, late protein expression, and virion assembly do not occur. It has been reported that transcripts corresponding to the immediate-early and early open reading frames (ORFs) ORF4, -21, -29, -62, -63, and -66 are present in neurons harboring latent VZV (9–13, 15, 25, 36, 50). Proteins expressed by these ORFs are present in the cytoplasm of latently infected neurons (9, 12, 15, 36, 49, 50). In particular, Lungu et al. demonstrated that ORF29p, a single-stranded DNA binding protein that is predominantly nuclear during lytic infection, is restricted to the cytoplasm of latently infected neurons in explanted human dorsal root ganglia (49). Upon reactivation, ORF29p accumulates in the nuclei of neurons undergoing productive infection (49). The detection of ORF29p and the other latency-associated proteins (LAPs) in the cytoplasm suggests a tight correlation between their nuclear import/exclusion and the progression of VZV lytic infection.

Most stages of the VZV life cycle that occur in vivo can be recapitulated in vitro. Cell-free VZV infection is lytic in primary human fibroblasts and MeWo cells, a melanoma-derived cell line. During lytic infection of these cell lines, ORF29p localizes predominantly to subnuclear compartments (39). Conversely, infection of cultured guinea pig enteric ganglia (EG) with cell-free VZV results in a latent infection and cytoplasmic localization of ORF29p in neurons (9). Latent VZV in EG cultures may be reactivated by superinfection with adenoviruses expressing ORF61p or HSV-1 ICP0. In response to this superinfection, ORF29p accumulates in the nuclei of infected cells (J. Chen et al., submitted for publication).

During lytic infection, ORF29p is expressed from a bidirectional 221-bp intergenic regulatory element that is shared with its divergently oriented neighboring gene, ORF28, which encodes the viral DNA polymerase (51, 53, 66). Transcription from ORF29 produces a predominant polyadenylated RNA transcript of 4.2 kb and a minor transcript of 4.1 kb (53). Transcription from both genes is tightly coordinated and requires VZV immediate-early protein ORF62p for efficient expression (51–53, 66). During latent infection, only the 4.2-kb transcript of ORF29 is detected, while the ORF28 transcript is absent (10, 15, 16, 50). Therefore, the ORF28 and ORF29

* Corresponding author. Mailing address: Department of Microbiology, 701 W. 168th St., New York, NY 10032. Phone: (212) 305-8149. Fax: (212) 305-5106. E-mail: sjs6@columbia.edu.

genes may, depending on the replication state of the virus, be expressed either synchronously or independently of each other. This differential transcription of only ORF29 during latency suggests a role for neuron-specific transcription factors in its regulation.

VZV ORF29 encodes a nonstructural 130-kDa, single-stranded DNA binding protein that is an orthologue of herpes simplex virus type 1 (HSV-1) ICP8 (39, 60). ORF29p and ICP8 share 50% sequence homology at the amino acid level. However, most of this similarity resides in the DNA binding motifs, while other areas of the proteins are less conserved. In addition to its presumed role in DNA replication, transfection assays have revealed that ORF29p can also influence transcription from some ORF62p-responsive promoters (3). No protein interaction data have been reported for ORF29p. It is not phosphorylated during lytic infection, despite the existence of multiple putative phosphorylation sites (14, 60). ORF29p modifications during latent infection have yet to be investigated.

The molecular basis for ORF29p localization during VZV infection is unclear. ORF29p lacks a classical nuclear import sequence, export signal, or any homology to ICP8 targeting sequences (39, 61, 64). We have shown that ORF29p nuclear import occurs independent of the presence of other VZV-specified proteins and that its nuclear localization sequence (NLS) maps to amino acids 9 to 154. The ORF29p NLS interacts either directly or indirectly with karyopherin α and shuttles into the nucleus via a Ran-dependent pathway, which is well conserved in most human cells (35, 42, 62). This, along with the observation that ORF29p enters the nuclei of infected neurons during reactivation, suggests that the mechanism governing nuclear import of ORF29p is not the determinant of its cell-type-specific localization.

In this report, we analyze the cellular localization patterns of ORF29p during VZV infection and during autonomous expression in MeWo cells, U373MG cells, and cultured guinea pig enteric neurons. We also investigate the effect of ORF61p and HSV-1 ICP0 expression on ORF29p localization and provide plausible explanations for the cell-type-specific localization pattern of ORF29p. Our results demonstrate that differential compartmentalization of ORF29p is cell type specific but can be influenced by subsequent expression of ORF61p or ICP0. In these cases, ORF61p or ICP0 induces nuclear accumulation of ORF29p in cell lines where it is normally cytoplasmic. Inhibition of the 26S proteasome, but not heat shock treatment, also affects the cellular distribution of ORF29p similarly to ICP0 expression. Fluorescence microscopy and pulse-chase experiments demonstrate that redistribution of ORF29p to the nucleus correlates with protein stabilization. Induced nuclear accumulation of ORF29p is also dependent on the novel ORF29p NLS that we have previously defined (62). Although proteasome inhibition induces ORF29p nuclear accumulation, this is not sufficient to reactivate latent VZV in EG cultures. A better understanding of the expression and localization of ORF29p could help elucidate the mechanisms controlling VZV latency.

MATERIALS AND METHODS

Mammalian cells. Human melanoma (MeWo) cells were maintained as monolayer cultures in Dulbecco's modified Eagle medium (DMEM) (GIBCO-BRL, Grand Island, NY) supplemented with 10% fetal bovine serum (Hyclone, Ogden, UT), 100 U/ml penicillin, and 100 μg/ml streptomycin (GIBCO-BRL) at 37°C in a 5% CO_2 atmosphere. 293A cells, a clonal derivative of HEK293 cells supplied by Frank Graham, and astrocytoma-derived U373MG cells were maintained under the same conditions except that the medium was supplemented with 5% Fetal-clone II (Hyclone). Twenty-four hours prior to infection, the cells were seeded onto coverslips in six-well tissue culture dishes for fluorescence microscopy assays or in 100-mm and 60-mm dishes for all other experiments. During virus infection, MeWo and U373MG cells were maintained in Eagle's minimal essential medium supplemented with 2% fetal bovine serum, 100 U/ml penicillin, and 100 μg/ml streptomycin.

Guinea pig enteric ganglia were isolated and cultured as previously described (9). In brief, ganglia were seeded for culture in two-well chamber slides that were coated with 10 μg/ml each of poly-D-lysine and mouse laminin in DMEM-F12 (GIBCO-BRL) supplemented with 2% fetal bovine serum, 100 U/ml penicillin, 100 μg/ml streptomycin, 100 μg/ml gentamicin, and 5.25 μg/ml amphotericin B (Fungizone). Mitotic inhibitors (10 μM 5-fluoro-2′-deoxyuridine, 10 μM uridine, and 1 μM cytosine β-D-arabinofuranoside) (Sigma, St. Louis, MO) were also added. Prior to virus infection, the mitotic inhibitors were removed, and the cells were subsequently cultured in their absence.

Viruses. (i) VZV. Jones VZV, a wild-type clinical isolate, was propagated in MeWo cell monolayers by serial passage of infected cells onto uninfected cells as described previously (26). Cell-free Jones VZV was obtained by infecting MeWo cells in 175-cm^2 tissue culture flasks until a cytopathic effect (CPE) was present. Infected cells were scraped in the maintenance medium and centrifuged at 577 × g for 10 min at 4°C in a Beckman CS-6KR refrigerated centrifuge. The cells were washed twice in cold phosphate-buffered saline (PBS) (1 mM KH_2PO_4, 10 mM Na_2HPO_4, 137 mM NaCl, 2.7 mM KCl, pH 7.4) before being resuspended in 1 ml of Hanks balanced salt solution per flask and sonicated twice for 30 s each. Cell debris was removed by centrifuging the lysed cells at 22 × g for 5 min at 4°C in a Tomy MX-160 high-speed refrigerated microcentrifuge. Cell-free virus stocks were stored in 0.5-ml aliquots at −80°C.

(ii) Adenoviruses. Adenovirus vectors MLP-0, Ad-0/125, and Ad-0/88 express HSV-1 ICP0, ICP0 with an insertion at amino acid 124, and ICP0 with an insertion at amino acid 697, respectively, under control of the adenovirus major late promoter (MLP) (67, 68). Adenoviruses AdORF29 and AdORF29ΔNLS express ORF29p and ORF29pΔNLS, respectively, under control of a mouse cytomegalovirus (mCMV) promoter and were constructed using a system (pDC516 and pBHGfrtΔE1,3FLP) that relied on FLP-mediated frt site recombination (Microbix Biosystems, Inc., Toronto, Ontario, Canada) (54). An empty adenovirus vector, Ad.MmCMV, was constructed by cotransfection of pDC516 and pBHGfrtΔE1,3FLP using the same system. Adenovirus AdORF61 expresses VZV ORF61p from the adenovirus MLP and was generated as described above. Viruses were plaque purified, stocks were produced, and titers were determined by fluorescent focus assays on 293A cells (58). All of the adenoviruses were propagated in 293A cells (24).

Proteasome inhibitor and cycloheximide treatment. Infected U373MG and MeWo cells were incubated in Eagle's minimal essential medium supplemented with 2% fetal bovine serum, 100 U/ml penicillin, 100 μg/ml streptomycin, and either dimethyl sulfoxide (DMSO) (Sigma), 20 μM MG132 (EMD Biosciences, La Jolla, CA) from a 10 mM stock in DMSO, 20 μM epoxomicin (EMD Biosciences) from a 1 mM stock in DMSO, or 50 μg/ml cycloheximide (Sigma) from a 10-mg/ml stock in water for the indicated period.

Plasmid construction. (i) ORF29 adenovirus vector construction. p29-12 and pZErO29ΔNLS were constructed as previously described (62). ORF29 was released from p29-12 by digestion with EcoRI and PmlI and cloned into the EcoRI and SmaI sites of pDC516 (Microbix Biosystems) to generate pDC516-29, which was cotransfected with pBHGfrtΔE1,3FLP (Microbix Biosystems) into 293A cells to generate AdORF29. An ORF29 gene containing a deletion in the NLS of nucleotides 459 to 821 was subcloned from pZErO29ΔNLS by using the same sites as for the full-length ORF29 fragment to generate pDC516ORF29ΔNLS, which was cotransfected with pBHGfrtΔE1,3FLP into 293A cells to produce AdORF29ΔNLS.

(ii) ORF61 adenovirus vector construction. The adenovirus MLP was released from pDS-2 (68) with SacII and HindIII and inserted into pBluescript II (Stratagene, La Jolla, CA) at the corresponding restriction enzyme sites to create pBS.MLP. pBS.MLP was digested with SacII, blunt ended with T4 DNA polymerase, and ligated with an EcoRI linker (New England Biolabs, Beverly, MA). VZV ORF61 was released from pGORF61 (33) by AccI digestion and subcloned into pDC511 at the AccI site. The adenovirus MLP was released from pBS.MLP by EcoRI and HindIII digestion and ligated into a pDC511 construct containing ORF61 that had been linearized using the same restriction enzymes. The resulting construct, pDC511.MLP.ORF61, was cotransfected with pBHGfrtΔE1,3FLP

into 293A cells to produce AdORF61. All vector inserts were verified by DNA sequencing.

Transfections. The plasmids pDC516-29, pDC516ORF29ΔNLS, pDC511.MLP.ORF61, and pBHGfrtΔE1,3FLP were cotransfected into 293A cells to make recombinant adenoviruses by using calcium phosphate precipitation as previously described (54).

Antibodies. Rabbit polyclonal antibodies against amino acids 1086 to 1201 of ORF29p and amino acids 765 to 868 of ORF62p were previously described (49). The mouse monoclonal antibody 1112 against HSV-1 ICP0 was purchased from the Goodwin Cancer Research Institute (Plantation, FL). A mouse monoclonal antibody to VZV gE was purchased from ViroStat (Portland, ME). Alexa Fluor 488-conjugated goat anti-mouse and Alexa Fluor 546 anti-rabbit antibodies were purchased from Molecular Probes (Carlsbad, CA). Goat anti-rabbit antibodies conjugated to horseradish peroxidase were purchased from KPL (Gaithersburg, MD).

Indirect immunofluorescence microscopy. Cells on glass coverslips were washed once with PBS, fixed for 25 min with 3.7% formaldehyde in PBS, washed two more times in PBS, and permeabilized with ice-cold acetone at −20°C for 10 min. Cells were washed twice more in PBS and blocked with 10% normal goat serum (Roche, Indianapolis, IN) in PBS plus 0.1% Tween 20 (Sigma, St. Louis, MO) (PBS-T) for 30 min. Cells were incubated with a 1:100 dilution of the appropriate primary antibody in 1% normal goat serum in PBS-T for 1 h and then washed three times for 5 min each in PBS-T. Cells were then incubated for 1 h with the appropriate Alexa Fluor-conjugated secondary antibody diluted 1:1,000 in 1% normal goat serum in PBS-T and washed once for 5 min with PBS-T, once for 10 min with PBS-T plus 0.5 μg/ml Hoechst 33258 (Sigma), and once again for 5 min in PBS-T. The coverslips were mounted with GEL/MOUNT (Biomeda, Foster City, CA).

All samples were visualized with a Zeiss Axiovert 200M inverted microscope, and images were acquired with a Zeiss Axiocam (Carl Zeiss Microimaging Inc., Thornwood, NY) by using Openlab 3.1 software (Improvision, Lexington, MA). Images were assembled with Adobe Photoshop (Adobe Systems Inc., San Jose, CA).

Pulse-chase metabolic labeling. Proteins were radiolabeled by first washing three times in PBS and starving the infected or control cell cultures of Met and Cys by incubating them with modified DMEM (GIBCO-BRL) for 30 min. Starvation medium was replaced with labeling medium supplemented with 1% dialyzed calf serum and 500 μCi/ml Tran^{35}S-label (ICN, Irvine, CA). After a 1-h pulse, cells were washed three times with PBS and incubated for the indicated chase time in normal growth medium before harvesting.

Immunoprecipitation. Radioactively labeled cells were harvested, washed twice with PBS, resuspended in 500 μl radioimmunoprecipitation (RIPA) lysis buffer (10 mM Na_2HPO_4 [pH 7.2], 150 mM NaCl, 1% Triton X-100, 0.5% sodium deoxycholate, 0.1% sodium dodecyl sulfate [SDS]) plus Complete protease inhibitor cocktail (Roche, Indianapolis, IN), and incubated on ice for 30 min. Cell extracts were clarified by centrifugation at 22,500 × g for 5 min at 4°C in a Tomy MX-160 high-speed refrigerated microcentrifuge. Proteins were immunoprecipitated overnight at 4°C with ORF29p antiserum conjugated to 50 μl of GammaBind Plus Sepharose beads (Amersham Biosciences). Beads were collected by centrifuging for 5 min at 400 × g at 4°C in a Tomy MX-160 high-speed refrigerated microcentrifuge and washed three times for 15 min each with RIPA buffer at 4°C. Immunoprecipitated proteins were released from beads by boiling in 50 μl PBS and 10 μl 6× SDS sample buffer (300 mM Tris-HCl [pH 6.8], 12% SDS, 0.6% bromophenol blue, 60% glycerol, 600 mM β-mercaptoethanol) for 10 min and subjected to SDS-polyacrylamide gel electrophoresis (SDS-PAGE).

Western blotting of cell lysates. Ten-centimeter dishes of infected MeWo and U373MG cells were harvested, washed twice with PBS, resuspended in 100 μl of RIPA lysis buffer plus Complete protease inhibitor cocktail (Roche), and incubated on ice for 30 min. Cell extracts were clarified by centrifugation at 22,500 × g for 5 min at 4°C in a Tomy MX-160 high-speed refrigerated microcentrifuge. Total protein concentration was measured using the Bio-Rad protein assay (Bio-Rad, Hercules, CA). Twenty microliters of 6× SDS sample buffer was added to the samples prior to boiling for 10 min and SDS-PAGE. The proteins were transferred to a nitrocellulose membrane (Schleicher & Schuell, Keene, NH) with a Bio-Rad Trans-Blot semidry apparatus before Western blotting. After blocking of the membrane in 4% nonfat milk in PBS-T, immobilized proteins were incubated with the ORF29p antibody at a 1:1,000 dilution in blocking solution for 1 h at room temperature. The membrane was washed three times in PBS-T, incubated with an anti-rabbit antibody conjugated to horseradish peroxidase at a 1:5,000 dilution in blocking solution for 1 h at room temperature, and washed again, and ORF29p was visualized by addition of the LumiGLO substrate (KPL) and exposure to X-ray film.

Northern blot analysis. Total RNA was isolated from infected MeWo and U373MG cells by using the TRIzol reagent (Invitrogen), Ten micrograms of total RNA was brought to 6 μl in diethyl pyrocarbonate-treated water and added to a solution of 1× MOPS (morpholinepropanesulfonic acid) (from a 10× stock; 0.2 M MOPS [pH 7.0], 20 mM sodium acetate, 10 mM EDTA [pH 8.0], 7.4% formaldehyde, 50% formamide, and 10 μg/ml of ethidium bromide). The samples were incubated at 85°C for 10 min, chilled on ice for 10 min, and combined with 1× formaldehyde gel loading buffer (from a 10× stock; 50% glycerol, 10 mM EDTA [pH 8.0], 0.25% [wt/vol] bromophenol blue, 0.25% [wt/vol] xylene-cyanol FF). The RNA was subjected to gel electrophoresis on a 1% agarose gel containing 2.2 M formaldehyde and 1× MOPS in 1× MOPS electrophoresis buffer. A 0.24- to 9.5-kb RNA ladder (Invitrogen) and the NEB RNA ladder (New England Biolabs, Beverley, MA) were run alongside the samples as molecular size markers. After photography, the gel was rinsed briefly in diethyl pyrocarbonate-treated water and incubated for 0.05 M NaOH for 20 min to partially hydrolyze the RNA. The gel was then washed in 20× SSC (3.0 M NaCl, 0.3 M sodium citrate, pH 7) for 40 min before transfer to a nylon membrane (Schleicher & Schuell) by standard upward capillary transfer. When the transfer was complete, the nylon membrane was rinsed in 2× SSC, and the RNA was UV cross-linked using the UV Stratalinker 2400 (Stratagene). The membrane was dried and prehybridized in 6× SSC, 0.5% SDS, 0.1 mg/ml salmon testis DNA, and 5× Denhardt's solution (from a 50× stock; 10% [wt/vol] bovine serum albumin, 25 mM Ficoll, 1% [wt/vol] polyvinylpyrrolidone) at 67°C for 2 h.

To make an ORF29-specific DNA probe, the EcoRI NotI fragment containing *ORF29* was excised from p29-12. Fifty nanograms of the released fragment or 50 ng of GAPDH (glyceraldehyde-3-phosphate dehydrogenase) mouse DECA-probe template (Ambion, Austin, TX) was added to a Boehringer Mannheim random-priming reaction mixture (Roche) in the presence of Redivue [α-^{32}P]dCTP (Amersham Biosciences). The samples were incubated at 37°C for 30 min before the reaction was stopped by incubation with 25 mM EDTA for 10 min at 65°C. The unincorporated nucleotides were removed with the QIAquick nucleotide removal kit (Qiagen, Valencia, CA), and the probes were boiled, added to the prehybridization buffer, and incubated with the membrane overnight at 67°C. The membrane was washed once at room temperature with 1× SSC and 0.1% SDS for 10 min and then three times at 67°C with 0.5× SSC and 0.1% SDS for 15 min each before being exposed to X-ray film. Prehybridization, hybridization, and washes were performed in a Techne Hybridizer HB-1D (Burlington, NJ).

RESULTS

Cell-type-dependent localization of ORF29p. Intracellular compartmentalization of ORF29p appears to correlate with the fate of VZV infection. Lytic infection of the dermis and epidermis during chicken pox and shingles results in predominantly nuclear accumulation of ORF29p, whereas ORF29p is predominantly cytoplasmic during latent infection of neurons in the dorsal root ganglia (49). We have previously shown that nuclear import of ORF29p occurs independently of other VZV proteins (62). To determine whether ORF29p nuclear exclusion results from interaction with VZV-specified proteins, an adenovirus (AdORF29) that expresses ORF29p was constructed. MeWo cells and cultured EG were infected with AdORF29 at a multiplicity of infection (MOI) of 50 (Fig. 1). The intracellular localization of ORF29p was assayed at 5 days postinfection (dpi) by indirect immunofluorescence (IF) microscopy. The nuclei in this experiment and all subsequent ones were visualized after counterstaining with Hoechst 33258. ORF29p expressed from AdORF29 localized to the nuclei of MeWo cells and the cytoplasm of cultured enteric neurons and enteric glia. This experiment demonstrates that localization of ORF29p is cell type specific and independent of other VZV-specified factors.

To facilitate further studies, a screen for continuous cell lines that exclude ORF29p from the nucleus during AdORF29 infection was performed. The survey revealed that ORF29p accumulates in the cytoplasm of U373MG cells, an astrocyte-

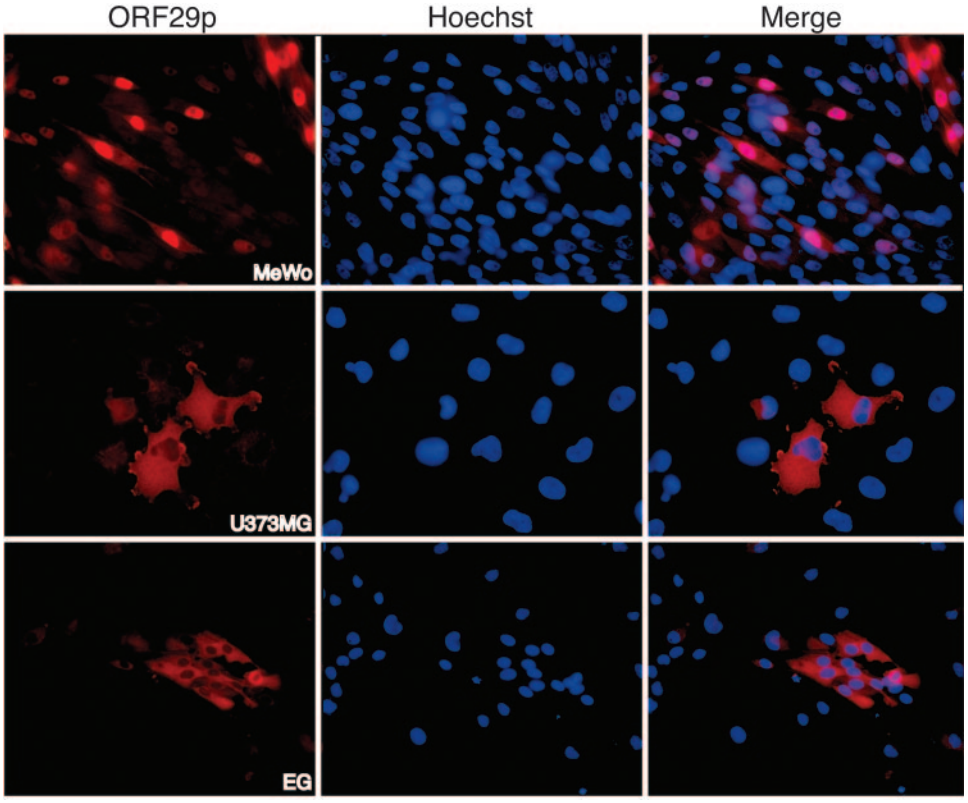

FIG. 1. Cellular localization of ORF29p. Cultured guinea pig EG, MeWo, and U373MG cells were infected with AdORF29 at an MOI of 50. The localization of ORF29p was examined at 5 dpi by indirect immunofluorescence microscopy. Nuclei were counterstained with Hoechst 33258.

like human cell line (Fig. 1), and also in rat C6 glioma cells. This result further supports a cell-type-specific localization pattern for ORF29p and provides a system for studying ORF29p nuclear exclusion in tissue culture. To verify that localization of ORF29p was not affected by adenovirus gene products, MeWo and U373MG cells were transfected with a plasmid that expresses only ORF29p. Immunocytochemical analysis of the distribution of ORF29p revealed a cell-type-specific localization pattern identical to that seen during AdORF29 infection. Western blotting was performed to verify that full-length ORF29p was expressed in each cell line (data not shown).

Localization of virus-specified proteins in cells infected with cell-free VZV. Infection of human fibroblasts and MeWo cells with cell-free VZV results in virus production, whereas infection of cultured EG results in latency (9, 62). ORF29p localization in these cases mimics what has been witnessed in vivo, in that ORF29p accumulates in the nucleus during lytic infection and in the cytoplasm during latency. Other hallmarks of lytic infection include nuclear distribution of the immediate-early gene product ORF62p and expression of the late protein gE (ORF68p). This is in contrast to the current model of latent infection, where the immediate-early protein ORF62p is excluded from the nucleus and late gene products are not detectable (9, 25, 40, 49).

MeWo cells, cultured EG, and U373MG cells were infected with cell-free VZV to determine whether both immediate-early and late proteins were expressed after infection of U373MG cells with cell-free VZV (Fig. 2). At 3 dpi, the cells were fixed and stained for ORF29p and gE (Fig. 2A), and ORF62p (Fig. 2B). Microscopic examination of VZV infected MeWo cells demonstrated cytopathic effects, nuclear accumulation of ORF29p, and expression of gE (Fig. 2A). In contrast, in enteric neurons infected with cell-free VZV, CPE was not detected, ORF29p and ORF62p were present only in the cytoplasm, and there was no detectable expression of gE (Fig. 2). This result mimics the localization pattern of ORF29p in human autopsy tissue (49).

Immunofluorescence studies revealed that infection of U373MG cells with cell-free VZV was lytic. In infected U373MG cells, CPE was evident, ORF29p and ORF62p were predominantly nuclear, and gE was expressed (Fig. 2). This corresponds with reports of lytic VZV infection of human primary astrocyte cultures (2, 37). Our data demonstrate that when ORF29p is expressed alone, it is cytoplasmic in U373MG cells; however, this cell line is unable to support latent VZV infection. This also indicates that the cell-type-dependent localization of ORF29p in U373MG cells is affected by expression of other VZV-specified proteins.

ORF29p localization is influenced by expression of HSV-1 ICP0 or VZV ORF61p. To investigate further the mechanisms involved in differential compartmentalization of ORF29p, we asked what herpesvirus proteins influenced ORF29p localization and how. Therefore, cultured guinea pig enteric neurons were inoculated with cell-free VZV to establish a latent infection (Fig. 3) (9). At 3 dpi, these cultures were superinfected with MLP-0 (67, 68) and incubated for an additional 48 h.

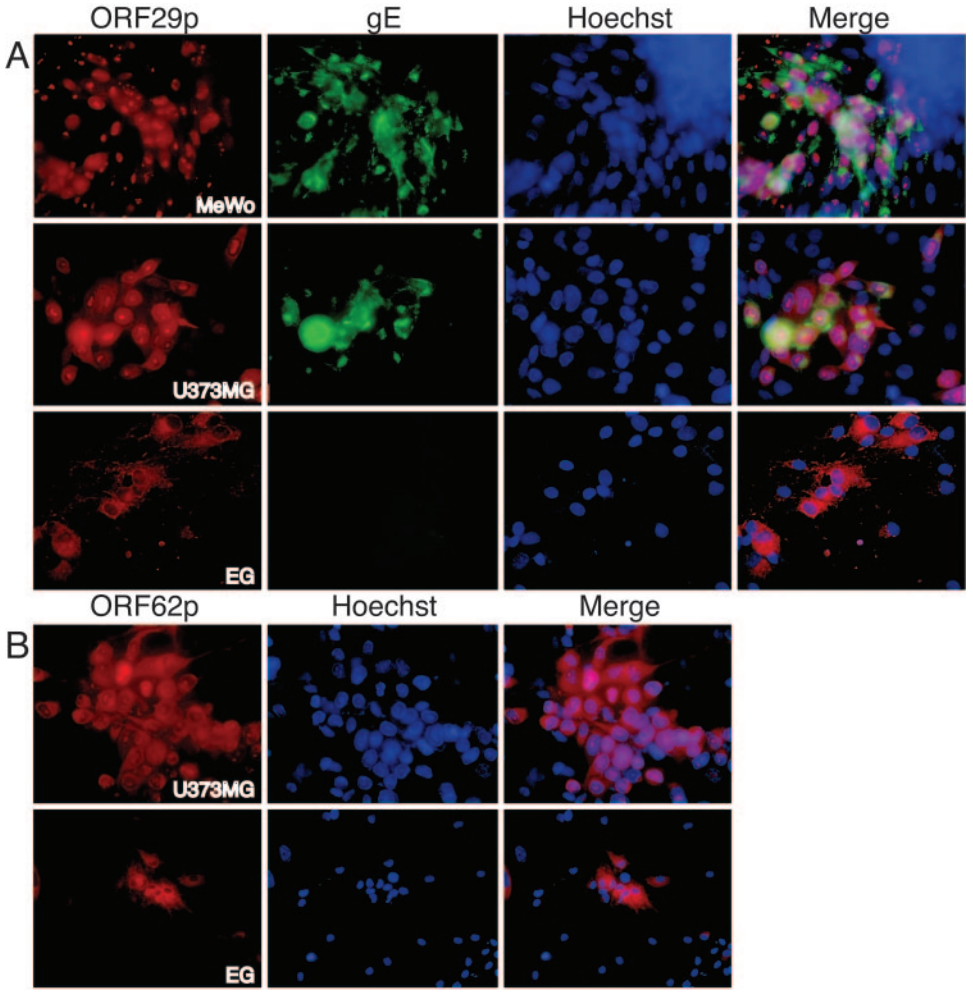

FIG. 2. Localization of virus-specified proteins in cells infected with cell-free VZV. Cultured EG, MeWo, and U373MG cells were infected with cell-free VZV at an MOI of 1. The expression and distribution of ORF29p and gE (A) and ORF62p (B) were examined at 3 dpi by indirect immunofluorescence microscopy.

VZV in neuron cultures that were superinfected with an empty adenovirus vector (Ad.MmCMV) remained latent as evident by the cytoplasmic localization of ORF29p and ORF62p and the absence of the late gene product gE (Fig. 3A). ICP0 expression appeared to reactivate latent VZV in enteric neurons, as evidenced by nuclear accumulation of ORF29p and ORF62p and expression of the late gene product gE in these cells (Fig. 3B). These same results were observed with an adenovirus expressing the VZV-encoded ICP0 homologue ORF61p (AdORF61) (Fig. 3C).

AdORF29, MLP-0, and AdORF61 were next used to determine whether expression of ICP0 or ORF61p was sufficient to alter the cellular distribution of ORF29p in cells autonomously expressing this VZV protein. Cultured EG and U373MG cells were infected with MLP-0 alone to determine the localization of ICP0 in these cell cultures (Fig. 4A). As previously demonstrated, ICP0 expressed from MLP-0 localized to the nucleus with punctate staining (67, 68). Following reactivation of latent VZV, ORF29p is found in the nuclei of neurons within human dorsal root ganglia (49) and cultured guinea pig enteric neurons (9). This observation raises the possibility that the sequence of ORF29p and ICP0 expression is important for relocalization. Therefore, to test the effect of ICP0 expression on localization of ORF29p, cultured EG and U373MG cells were first infected with AdORF29, and after 3 days the cells were superinfected with MLP-0 and incubated for an additional 48 h. The cultures were then fixed, and the distributions of ORF29p and ICP0 were determined by indirect IF. Sequential expression of ICP0 following ORF29p expression results in nuclear accumulation of ORF29p in cultured enteric neurons and U373MG cells (Fig. 4B). Thus, after ORF29p expression is established, expression of ICP0 is able to induce a change in the subcellular localization of ORF29p. In contrast, expression of ICP0 had no effect on ORF29p distribution in MeWo cells (data not shown).

These experiments were repeated using AdORF61, and similar results were obtained. Expression of ORF61p following cytoplasmic accumulation of ORF29p results in nuclear import of ORF29p (Fig. 4D). Without a monoclonal antibody to ORF61p, we were unable to verify the coexpression of ORF29p and ORF61p in the same cells. The fact that both VZV ORF61p and HSV-1 ICP0 can affect ORF29p subcellular

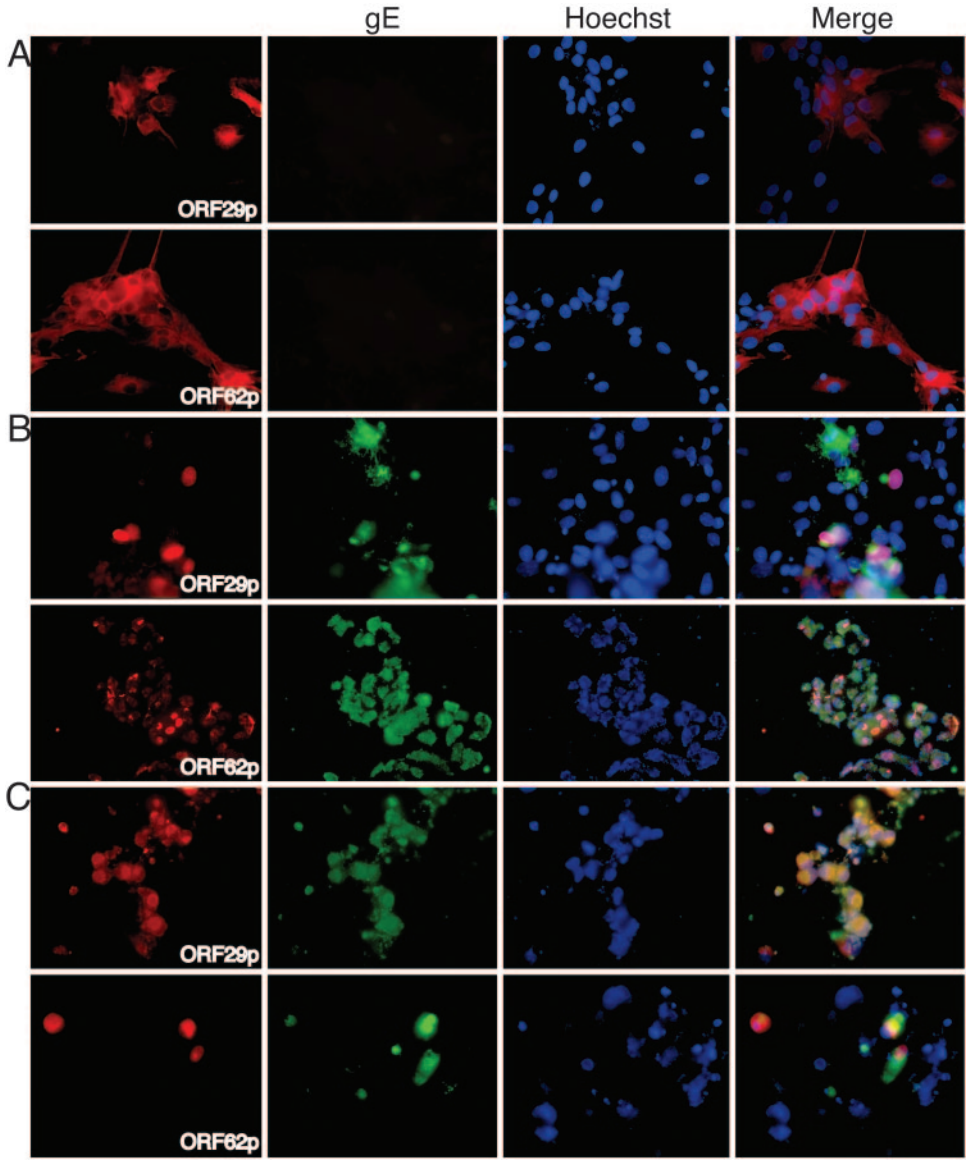

FIG. 3. Localization of viral proteins in VZV-infected guinea pig EG. Cultured EG were infected with cell-free VZV at an MOI of 1. At 3 dpi, cells were superinfected with either Ad.MmCMV (A), MLP-0 (B), or AdORF61 (C) at an MOI of 50 for 48 h prior to analysis by indirect immunofluorescence. ORF29p, ORF62p, and gE were detected after incubation with specific antisera.

distribution suggests that they have conserved the activity required for translocation.

In other studies we have established that the ORF29p NLS lies between amino acids 9 and 154 and that deletion of amino acids 153 to 272 abrogates ORF29p nuclear import (62). The requirement for this novel NLS for nuclear translocation of ORF29p in U373MG cells and EG was examined. EG, U373MG, and MeWo cells were infected with AdORF29ΔNLS, which expresses a protein that lacks an active NLS and therefore accumulates exclusively in the cytoplasm (Fig. 4E) (62). The effect of ICP0 expression on the localization of ORF29pΔNLS was also investigated. Cultured EG and U373MG cells were infected as described above, and the intracellular distributions of ORF29pΔNLS and ICP0 were analyzed by indirect IF. The NLS mutant protein remains cytoplasmic even after expression of ICP0 (Fig. 4C). Thus, the nuclear accumulation of ORF29p in cultured EG and U373MG cells induced by ICP0 expression utilizes the same NLS required for ORF29p nuclear import during lytic infection.

ICP0 exon 2 and 3 mutants are not able to affect ORF29p intracellular distribution. ICP0 is a multifunctional protein that affects the expression of many viral and cellular gene products (4, 17, 20, 21, 23, 27, 30, 34, 46, 48, 55–57, 67). To determine more precisely the effect of ICP0 expression on ORF29p localization, the regions of ICP0 involved in ORF29p redistribution were investigated using ICP0 mutant adenoviruses, Ad-0/125 and Ad-0/88, previously characterized in our laboratory (67). Ad-0/125 and Ad-0/88 are linker insertion mutants that have five amino acid insertions at positions 124 and 697 of the ICP0 protein, respectively. The insertion at amino acid 124 falls within the zinc finger domain in exon 2 and

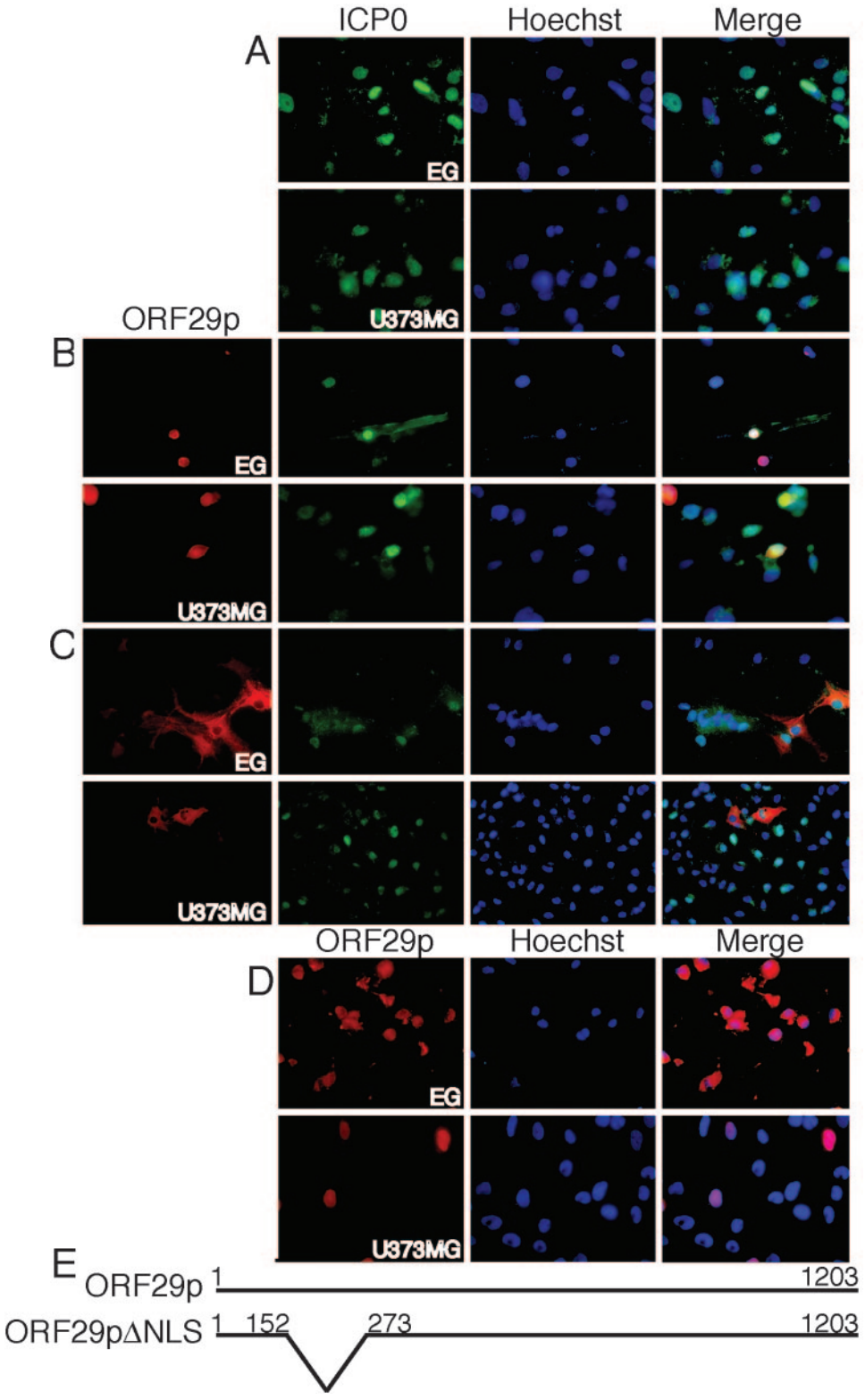

FIG. 4. Localization of ORF29p in cells expressing ORF29p and HSV-1 ICP0 or VZV ORF61p. (A) Cultured EG and U373MG cells were infected with MLP-0 at an MOI of 50. ICP0 was detected at 5 dpi by indirect immunofluorescence microscopy after incubation with specific antiserum. (B to D) EG and U373MG cells were also infected with either an adenovirus expressing the wild-type ORF29p (AdORF29) (B and D) or an adenovirus expressing a mutant ORF29p with a deletion in the NLS (AdORF29ΔNLS) (C) at an MOI of 50. After 72 h, the EG and U373MG cells were superinfected with MLP-0 (B and C) or AdORF61 (D) at an MOI of 50. The cultures were incubated for another 48 h before the distributions of ORF29p, ORF29pΔNLS, and ICP0 were examined by indirect immunofluorescence microscopy. (E) Schematic of the amino acids deleted from the ORF29pΔNLS mutant.

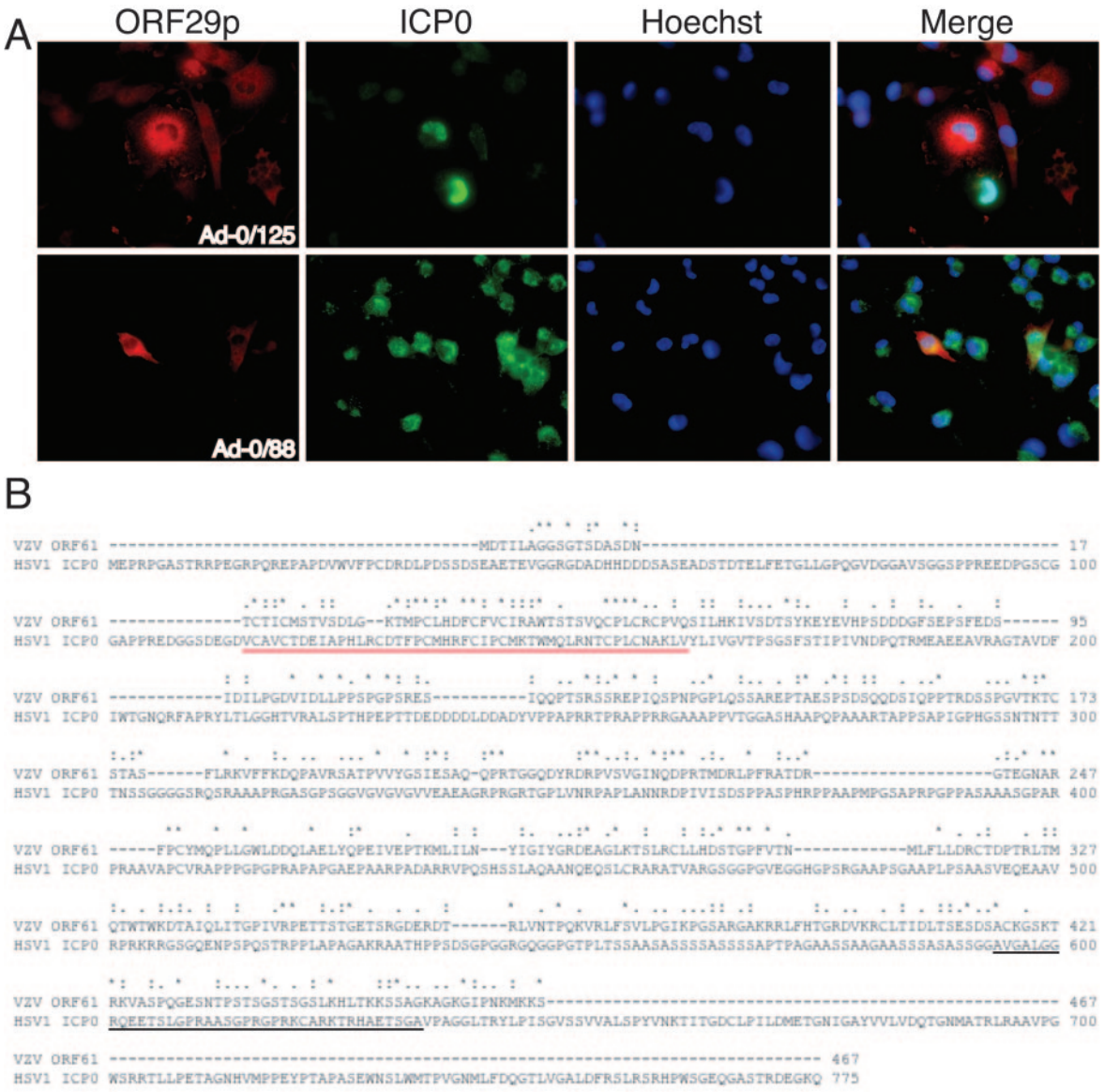

FIG. 5. Localization of ORF29p in cells after sequential expression of HSV-1 ICP0 insertion mutants. (A) U373MG cells were infected with AdORF29 at an MOI of 50. After 72 h, the cells were superinfected with either Ad-0/125 or Ad-0/88 at an MOI of 50. The cultures were incubated for another 48 h before the distributions of ORF29p and ICP0 variants were examined by indirect immunofluorescence microscopy. (B) Clustal X alignment of HSV-1 ICP0 (accession no. P08393) and VZV ORF61p (accession no. P09309) amino acid sequences. The underlines mark the functional domains as characterized in ICP0. The red underline denotes the RING finger motif encoded by exon 2 that possesses E3 ubiquitin ligase activity as well as binds the cdc34 E2 ubiquitin-conjugating enzyme; this domain is well conserved between the two proteins. The black underline identifies the domain that confers E3 ubiquitin ligase activity on HSV-1 ICP0; note that this domain is not well conserved between these proteins. The asterisks identify positions that have a single, fully conserved residue, the colons identify highly conserved residues, and the periods identify weakly conserved residues at the indicated positions.

eliminates ICP0 transactivation and reactivation activity. The insertion at position 697 lies in exon 3 and had no effect on ICP0's ability to activate transcription or reactivate latent HSV (8, 67). U373MG cells were first infected with AdORF29, and 3 days later the cells were superinfected with Ad-0/125 and Ad-0/88 and incubated for an additional 48 h. The cells were fixed, and the distributions of ORF29p and ICP0 were determined by indirect IF. The ICP0 proteins expressed by Ad-0/125 and Ad-0/88 localized to the nuclei of infected U373MG cells, but they were unable to target ORF29p to the nucleus in cells coexpressing both proteins (Fig. 5A). This differs from the case for wild-type ICP0, which when expressed in cells containing ORF29p results in nuclear accumulation of the latter. Superinfection with Ad-0/125 and Ad-0/88 had no effect on ORF29p localization in MeWo cells (data not shown).

Pathways known to involve ICP0 exons 2 and 3 were investigated for their effect on ORF29p. One cellular system utilized by ICP0 to influence protein abundance is the ubiquitin-dependent proteasome degradation pathway (4, 17, 46, 57). The portion of ICP0 encoded by exon 2 contains a RING finger

motif that confers E3 ubiquitin ligase activity and binds the cdc34 E2 ubiquitin-conjugating enzyme. Additionally, the region of ICP0 encoded by exon 3, which does not contain a RING finger, also possesses E3 ubiquitin ligase activity. Amino acids 594 to 633 of the region encoded by exon 3 bind herpesvirus-associated ubiquitin-specific protease, which is involved in deubiquitination of target proteins. ICP0 also dynamically associates with proteasome complexes, and this interaction is stabilized by inhibition of proteasomal activity (5, 17, 28, 65). Proteasome activity and ubiquitination are also implicated in directing the subcellular localization of other molecules, such as HSV-1 UL9 and p53 (18, 19, 47). Although ORF61p has not been demonstrated to be involved in the proteasome pathway, Clustal X analysis reveals that the HSV-1 ICP0 RING finger motif that confers E3 ubiquitin ligase activity and binds the cdc34 E2 ubiquitin-conjugating enzyme is highly conserved in VZV ORF61p (Fig. 5B). The motif in ICP0 encoded by exon 3 that possesses E3 ubiquitin ligase activity and dynamically associates with the proteasome is not conserved in ORF61p.

Effect of proteasome inhibitors on ORF29p localization. Given the requirement for the exon 2 and 3 domains of ICP0 to localize ORF29p to the nucleus in U373MG cells, we asked whether proteasome activity is involved in nuclear translocation. Cultured EG, U373MG, and MeWo cells infected with AdORF29 were treated at 3 dpi with 20 μM MG132 or DMSO for 6 h before analysis of the intracellular distribution of this protein by indirect IF. MG132 is a peptide aldehyde that potently, but reversibly, inhibits the chymotrypsin-like activity of the 26S proteasome (41, 44). Following inhibition of proteasome activity, ORF29p accumulates in the nuclei of cultured enteric neurons and U373MG cells, while addition of DMSO has no effect on ORF29p localization in either cell type (Fig. 6). MG132 treatment had no effect on ORF29p localization in the nuclei of MeWo cells (Fig. 6C).

MG132 does not exclusively target the proteasome but also inhibits some lysosomal cysteine proteases, calpains, and serine proteases of digestive vacuoles (41, 44). To verify that the accumulation of ORF29p in the nucleus was a function of the inhibition of proteasome activity, U373MG cells infected with AdORF29 were treated at 3 dpi with 20 μM epoxomicin for 6 h before IF analysis. Epoxomicin, an epoxyketone, is more selective than MG132 in that it targets all three catalytic activities of the 26S proteasome without affecting other proteases (41, 44). Treatment with epoxomicin recapitulated the results seen with MG132, in that ORF29p accumulates in the nuclei of U373MG cells infected with AdORF29 (Fig. 6B). The finding that two different proteasome inhibitors induce nuclear accumulation of ORF29p supports a role for the proteasome in the redistribution of ORF29p to the nuclei of cultured EG and U373MG cells.

The cytoplasmic localization of ORF29pΔNLS is unaffected in U373MG cells treated with epoxomicin (Fig. 6D). We surmise from these results that proteasome inhibitor-induced ORF29p nuclear accumulation in U373MG cells uses the NLS that we previously defined for nuclear import in all cell types examined (62).

Blocking of protein degradation with proteasome inhibitors leads to a buildup of ubiquitinated, misfolded, and damaged proteins. This in turn triggers the heat shock response, which alters the cell environment and thereby makes interpretation of proteasome inhibition data difficult (41, 44). Therefore, we next asked if heat shock was able to alter the localization of ORF29p. U373MG and MeWo cells were infected with AdORF29 at an MOI of 50. At 3 dpi, infected cells were incubated at 42°C for 30 min and allowed to recover for 1 h at 37°C prior to fixing and staining for ORF29p localization. Heat shock treatment did not alter ORF29p localization in either cell line, indicating that the heat shock response is not sufficient to relocate ORF29p into the nuclei of U373MG cells (data not shown).

ORF29p is less stable in the cytoplasm than in the nuclei of U373MG and MeWo cells. The alteration of ORF29p subcellular localization in cultured EG and U373MG cells in response to proteasome inhibition raised the question of whether the protein's stability contributed to its cellular compartmentalization. To investigate this, U373MG and MeWo cells infected with AdORF29 were treated at 3 dpi with either DMSO or 50 μg/ml of cycloheximide for 6 h to inhibit protein translation. Cells were fixed, and ORF29p localization was examined by IF analysis (Fig. 7). Following cycloheximide treatment, the intensity of the cytoplasmic signal from ORF29p diminished in U373MG cells but not in MeWo cells, where the strong signal in the nucleus remained.

To determine whether the nuclear localization of ORF29p following inhibition of the proteasome resulted from de novo protein synthesis or protein stabilization, U373MG cells were infected with AdORF29 and treated at 3 dpi with MG132 and cycloheximide for 6 h before the cells were examined for the intracellular distribution of ORF29p (Fig. 7A). Inhibition of both proteasome activity and protein synthesis allowed for nuclear accumulation of stabilized ORF29p. The cycloheximide experiments suggest that ORF29p has a shorter half-life in U373MG cells than in MeWo cells and that de novo translation of ORF29p is not required for relocalization in U373MG cells following MG132 treatment.

Two biochemical experiments were done to correlate the abundance and stability of ORF29p in the different cell types with its localization pattern. First, MeWo and U373MG cells were infected with AdORF29 at an MOI of 50, and at 3 dpi the infected cultures were either mock treated, treated with MG132, or treated with cycloheximide for 6 h. Cell lysates were prepared and analyzed by Western blotting for ORF29p (Fig. 8). The total protein loaded into each well was normalized by correcting for the abundance of a nonspecific protein band that cross-reacts with the antibody to ORF29p. The change in abundance of ORF29p in MeWo and U373MG cells was calculated as the percentage of protein present in the mock-treated samples (Fig. 8). Analysis of the ORF29p level following these treatments reveals that it more than doubled after MG132 treatment of U373MG cells and decreased by 25% when protein synthesis was inhibited. ORF29p levels in MeWo cells increased slightly after MG132 and cycloheximide treatment, but not to the same extent as seen in U373MG cells. Thus, ORF29p is less stable in U373MG cells than in MeWo cells, and this stability is affected by inhibition of the proteasome and translation. The increased stability of ORF29p in U373MG cells following MG132 treatment also correlates with its appearance in the nucleus.

In the second set of experiments, pulse-chase analyses were conducted to determine the half-life of ORF29p in MeWo and

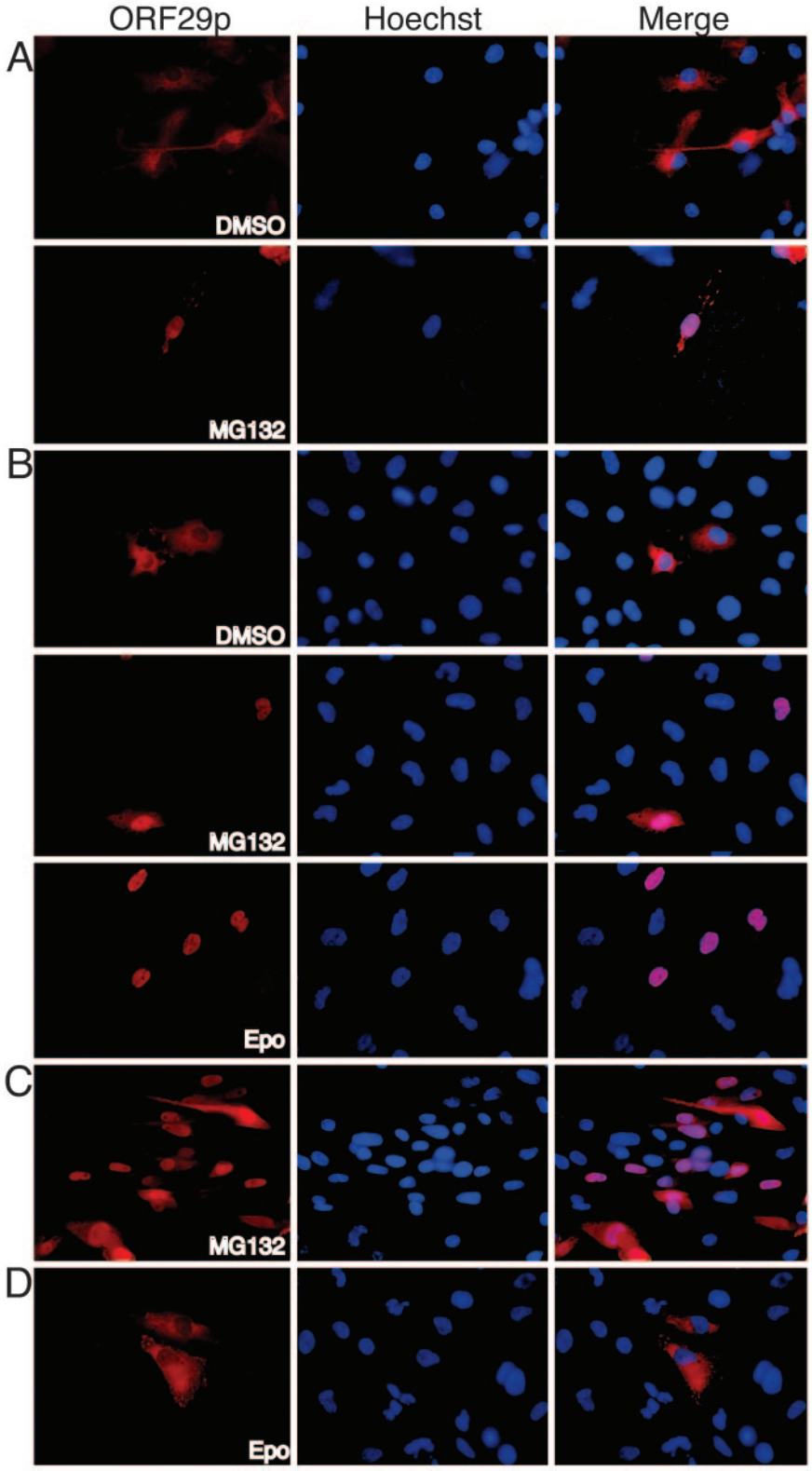

FIG. 6. Localization of ORF29p in cells treated with proteasome inhibitors. (A to C) Cultured EG (A), U373MG (B), and MeWo (C) cells grown on glass coverslips were infected with AdORF29 at an MOI of 50. (D) U373MG cells were infected with AdORF29ΔNLS at an MOI of 50. At 3 dpi, infected cultures were treated with either DMSO, 20 μM MG132, or 20 μM epoxomicin (Epo) for 6 h prior to analysis. ORF29p and ORF29pΔNLS were detected by indirect immunofluorescence microscopy after incubation with antiserum specific for ORF29p.

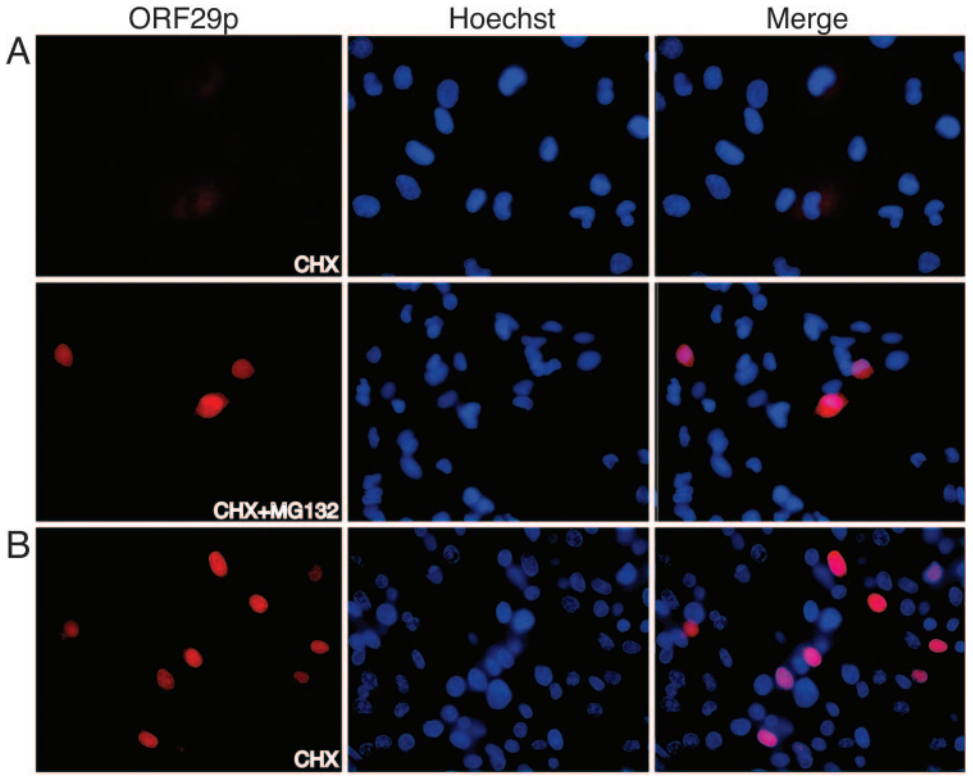

FIG. 7. Localization of ORF29p in cells treated with cycloheximide. U373MG (A) and MeWo (B) cells grown on glass coverslips were infected with AdORF29 at an MOI of 50. At 3 dpi, infected cultures were treated with 50 μg/ml of cycloheximide (CHX) or with 50 μg/ml cycloheximide and 20 μM MG132 for 6 h and fixed. ORF29p was detected by indirect immunofluorescence microscopy after reaction with specific antisera.

U373MG cells. These cell lines were infected with AdORF29 and incubated for 3 days in maintenance medium, after which they were washed and starved for 30 min in labeling medium containing either DMSO or MG132 before the addition of a similar medium containing Tran^{35}S-label. After a 1-h pulse, the labeling medium was removed and cells were washed and incubated in complete medium containing either DMSO or MG132 for the indicated chase times. Cell extracts were prepared by lysis in RIPA buffer, and the lysates were normalized for whole-cell protein concentration before immunoprecipitation of ORF29p. Bound proteins were subjected to SDS-PAGE analysis and visualized by autoradiography (Fig. 9). Changes in protein levels were determined relative to the levels of the 0-h chase time points (Fig. 9 and 10). In the presence and absence of MG132, labeled ORF29p is stable throughout the 6-h chase period in MeWo cells (Fig. 9A). In other studies, ORF29p was shown to be stable in fibroblasts even after a 24-h chase (data not shown). However, in DMSO-treated U373MG cells, labeled ORF29p was not detectable after 6 h (Fig. 9B). By contrast, when the proteasome was inhibited with MG132, 66% of ORF29p remained after a 6-h chase. These experiments support the results of the IF analyses that showed that ORF29p is more stable when accumulated in the nucleus than when it is present only in the cytoplasm. At the 6-h chase time point in MeWo cells, bands larger and smaller than ORF29p appear on the autoradiograph and are less intense in the samples treated with MG132 (Fig. 9A). Protein species with these same molecular weights are also seen at all chase time points in U373MG cells and are also more abundant at later times in untreated cells (Fig. 9B). These larger and smaller ORF29p-related species are also seen in the Western blot analyses shown in Fig. 8. They may represent modification and degradation products, respectively.

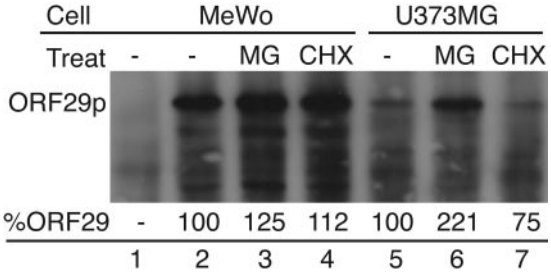

FIG. 8. Western blot analysis of ORF29p after treatment with MG132 or cycloheximide. MeWo and U373MG cells were infected with AdORF29 at an MOI of 50 (lanes 2 to 7) or mock infected (lane 1). At 3 dpi, cells were treated with either 20 μM MG132 (MG) (lanes 3 and 6), 50 μg/ml cycloheximide (CHX) (lanes 4 and 7), or DMSO (lanes 1, 2, and 5) for 6 h. Cells were harvested, lysed in RIPA buffer, and subjected to SDS-PAGE on an 8% gel. Proteins were transferred to a nitrocellulose membrane, reacted with specific antisera, and visualized using an horseradish peroxidase reporter substrate. Band intensity (percent ORF29) was quantified relative to ORF29p levels in the DMSO-treated sample by using the ImageJ program, and total protein levels per well were normalized against a band that represents a cross-reacting protein that was detected in all lanes.

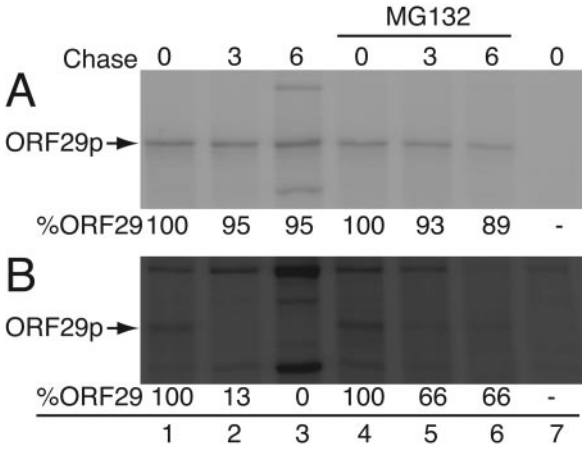

FIG. 9. Autoradiograph of metabolically labeled ORF29p. MeWo (A) and U373MG (B) cells were infected with AdORF29 at an MOI of 50 (lanes 1 to 6) or mock infected (lane 7). At 3 dpi, cells were labeled with 500 μCi/ml Tran^{35}S-label for 1 h in the presence of either 20 μM MG132 (lanes 4 to 6) or DMSO (lanes 1 to 3 and 7). The labeling medium was replaced with DMEM supplemented with 10% fetal bovine serum and either 20 μM MG132 (lanes 4 to 6) or DMSO (lanes 1 to 3 and 7) for the indicated chase times. Cells were harvested and lysed in RIPA buffer, and ORF29p was immunoprecipitated and subjected to analysis by SDS-PAGE on an 8% gel. Proteins were visualized by autoradiography. Band intensity was quantified using the ImageJ program, and total protein levels per well were normalized as described in the legend to Fig. 8. Percent ORF29 was calculated relative to the amount present at the 0-h chase time point.

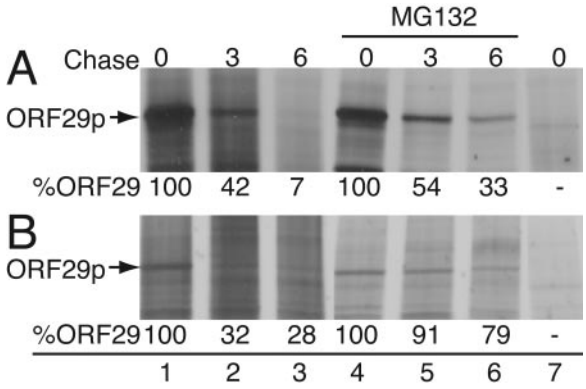

FIG. 10. Autoradiograph of metabolically labeled ORF29pΔNLS. MeWo (A) and U373MG (B) cells were infected with AdORF29ΔNLS at an MOI of 50 (lanes 1 to 6) or mock infected (lane 7). At 3 dpi, cells were labeled with 500 μCi/ml Tran^{35}S-label for 1 h in the presence of either 20 μM MG132 (lanes 4 to 6) or DMSO (lanes 1 to 3 and 7). The labeling medium was replaced with DMEM supplemented with 10% fetal bovine serum and either 20 μM MG132 (lanes 4 to 6) or DMSO (lanes 1 to 3 and 7) for the indicated chase time. Cells were harvested, lysed in RIPA buffer, immunoprecipitated with ORF29p-specific antiserum, and subjected to SDS-PAGE analysis on an 8% gel. Proteins were visualized by autoradiography. Band intensity was quantified using the ImageJ program, and total protein levels per well were normalized against a nonspecific band detected in all lanes. Percent ORF29pΔNLS (%ORF29) was calculated relative to the amount present at the 0-h chase time point.

Another pulse-chase experiment was performed with AdORF29ΔNLS-infected MeWo and U373MG cells to determine whether nuclear import was necessary for the survival of ORF29p in MeWo cells. Figure 10A demonstrates that ORF29pΔNLS was almost completely degraded after a 6-h chase in MeWo cells, and treatment with MG132 was able to stabilize only 33% of the protein. ORF29pΔNLS was more stable than the wild type in DMSO-treated U373MG cells, but only 32% of the protein remained after a 6-h chase (Fig. 10B). Like its wild-type protein counterpart, ORF29pΔNLS was stabilized when proteasome activity was inhibited in U373MG cells. The fact that ORF29pΔNLS is unstable in MeWo cells suggests that ORF29p needs to reach the nucleus to survive.

Analysis of ORF29 mRNA from AdORF29-infected cells. The pulse-chase experiments demonstrate that ORF29p is stabilized in U373MG cells after treatment with MG132. These experiments, however, do not exclude the possibility that inhibition of the proteasome up-regulated transcription factors, resulting in increased accumulation of the RNA encoding ORF29p. Northern blot analysis of ORF29 mRNA from AdORF29 or VZV infection of MeWo and U373MG cells was done to investigate this point. ORF29 mRNA from both adenovirus- and VZV-infected cells resolved as a single species of 4.2 kb under the conditions of our analysis (data not shown). In a previous report, Meier et al. stated that during lytic infection of fibroblasts, ORF29 is transcribed as two species that migrate at 4.1 and 4.2 kb (50). In that study, transcription of ORF29 was shown to initiate at two sites. An mCMV promoter drives the adenovirus expression cassette used in the current study, and therefore only a single RNA species is predicted. Interestingly, when MeWo and U373MG cells infected with AdORF29 were treated with MG132 for 6 h, the ORF29 RNA levels increased in both cell lines while the level of GAPDH RNA remained constant. The percent increase in ORF29 RNA levels between treated and untreated samples was similar in MeWo and U373MG cultures. This result does not account for the twofold increase in protein levels observed following MG132 treatment of U373MG but not MeWo cells (Fig. 8). Thus, the increase in ORF29 RNA levels is not sufficient to account for the accumulation of protein in U373MG cells.

MG132 reversal induces ORF29p degradation and accumulation of de novo protein in the cytoplasm. To determine whether nuclear translocation protected ORF29p from proteasome degradation, we took advantage of the fact that the action of MG132 is reversible (41, 44). At 3 dpi with AdORF29, U373MG cells were treated for 6 h with MG132. The cells were then washed and incubated for an additional 6 h in normal growth medium containing either DMSO or 50 μg/ml of cycloheximide (Fig. 11). Immunofluorescence microscopy demonstrated that ORF29p accumulated in the cytoplasm of U373MG cells when the inhibitory activity of MG132 was reversed. If protein synthesis was inhibited during and after reversal, ORF29p was cytoplasmic but barely detectable. Thus, the accumulation of ORF29p in the cytoplasm results from de novo synthesis, and nuclear ORF29p that amasses during treatment with MG132 is subsequently either degraded in situ or exported to the cytoplasm and destroyed. There are no reports on whether ORF29p shuttles, although leptomycin B has no effect on ORF29p localization in U373MG cells (data not shown). However, this observation only rules out the involvement of a CRM1-dependent export pathway (29, 43).

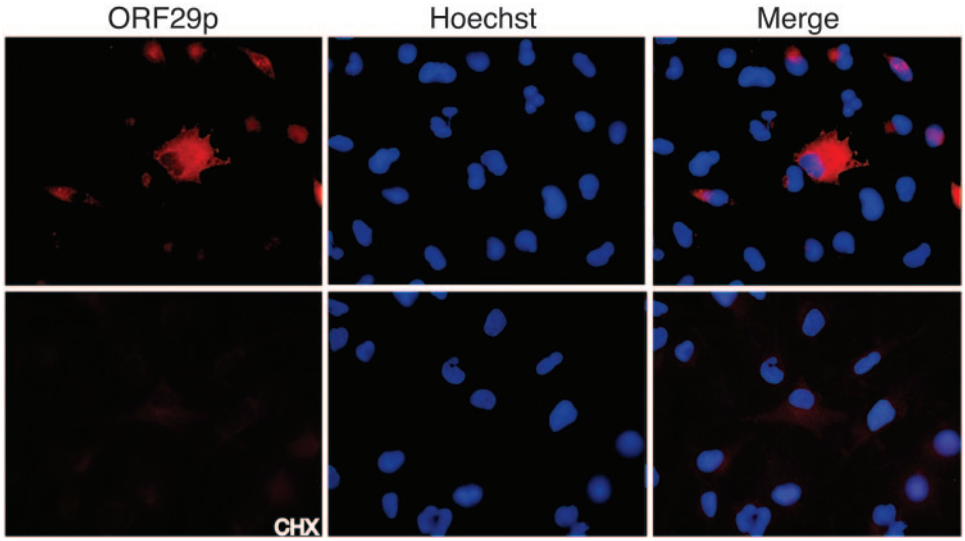

FIG. 11. Localization of ORF29p in U373MG cells after MG132 reversal. U373MG cells grown on coverslips were infected with AdORF29 at an MOI of 50. At 3 dpi, infected cultures were treated with 20 μM MG132. After 6 h, the cells were washed three times in PBS and the medium was replaced with either DMEM supplemented with 10% fetal bovine serum or DMEM supplemented with 10% fetal bovine serum and 50 μg/ml of cycloheximide (CHX) for 6 h and then fixed in situ. ORF29p was detected by indirect immunofluorescence microscopy after incubation with specific antisera.

Inhibition of the proteasome targets ORF29p to the nuclei of cultured enteric neurons harboring latent VZV but does not reactivate the virus. It was of interest to determine what effect inhibition of the proteasome had on ORF29p and other VZV-specified proteins during latent infection of cultured neurons. MG132 was previously shown to affect HSV-1 replication, ICP0 transactivation activity, and HSV-1 reactivation from latently infected cells (22, 59). These findings are not surprising, as during HSV-1 infection, the proteasome is involved in the disruption of cellular nuclear domains 10 and formation of viral replication compartments (4, 6, 7). An active proteasome is also essential for ICP0-mediated targeting of NF-κB to the nuclei of infected cells, which then up-regulates NF-κB-responsive genes that may aid in viral replication (17).

To determine whether the subcellular location of the latency-associated proteins was altered by inhibition of the proteasome and to determine if the virus was reactivated in response to the drug, latently infected enteric neurons were either mock treated, superinfected with MLP-0, or treated with 20 μM MG132. The cells were fixed and scored for the expression of ORF29p, ORF62p, and gE by IF analysis (Fig. 3 and 12A). As expected, VZV infection remained latent in mock-treated cells, as demonstrated by the presence of ORF29p and ORF62p in the cytoplasm and the absence of gE (Fig. 12). Superinfection of cultures with MLP-0 reactivated latent VZV in cultured enteric neurons as judged by the presence of ORF29p and ORF62p in the nucleus and expression of gE (Fig. 3). MG132 treatment of latently infected EG resulted in nuclear accumulation of ORF29p without gE expression (Fig. 12A). The absence of gE and CPE indicates that while inhibition of the proteasome results in nuclear import of ORF29, it is not sufficient to reactivate VZV. Moreover, treatment with MG132 did not affect ORF62p localization in latently infected neurons (Fig. 12A). Thus, nuclear localization of ORF29p can occur independent of translocation of the other LAPs.

Because MG132 affects the cell in many ways, we asked whether reversal of the action of MG132 in cells where ORF29p was nuclear would result in reactivation of latent VZV. To investigate this point, cultured enteric neurons harboring latent VZV were treated with MG132 for 6 h. The neurons were then washed and incubated in normal maintenance medium for an additional 18 h before being fixed. IF analysis of these cultures illustrates that after reversal of MG132, ORF29p disappears from the nucleus and accumulates in the cytoplasm of expressing neurons, while VZV remains latent (Fig. 12B). This correlates with data from similar MG132 reversal experiments done with U373MG cells and supports the observation that nuclear import of ORF29p following inhibition of the proteasome is not sufficient to reactivate latent VZV (Fig. 12B).

DISCUSSION

Maintenance of latency is critical for the establishment of lifelong persistence of VZV. VZV is novel among alphaherpesvirus in that during latency, immediate-early and early ORF4, -21, -29, -62, -63, and -66 appear to be expressed and their subcellular distribution correlates with the state of infection (9, 12, 15, 36, 49, 50). These proteins are retained in the cytoplasm during latency until the block to the remainder of viral genomic expression is broken (31), and then they accumulate in the nucleus. This observation indicates that confinement of VZV LAPs to the cytosol may be critical for maintaining quiescence. However, while the LAPs appear to accumulate in the cytoplasm rather than the nucleus, the possibility that some protein is present in the nucleus below the levels of detection or shuttles between the nucleus and cytoplasm cannot be ruled out.

Whether the expression and cytoplasmic localization of the VZV LAPs during latent infection is a consequence of related

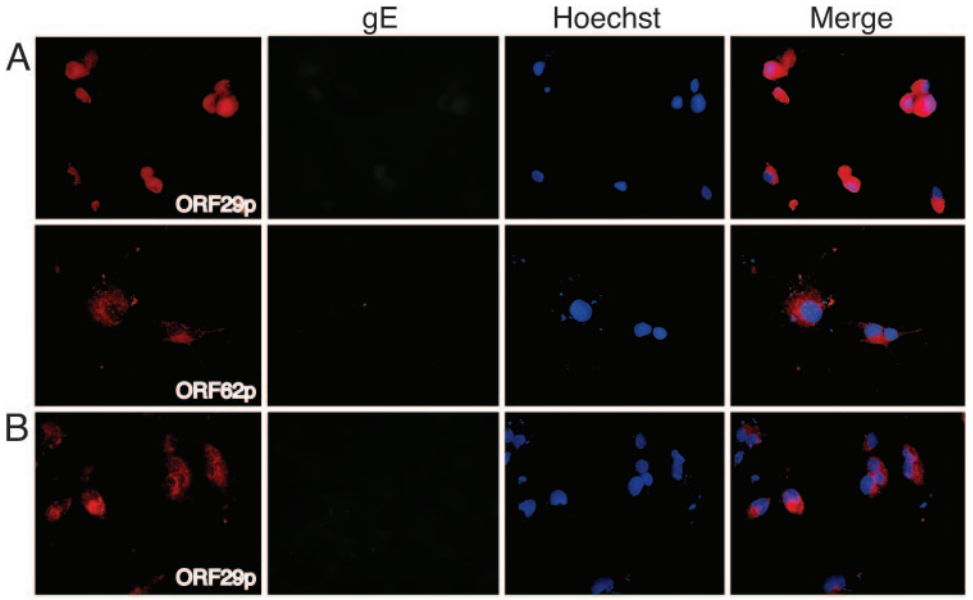

FIG. 12. Localization of viral proteins in VZV-infected guinea pig EG treated with proteasome inhibitors. Cultured EG were infected with cell-free VZV at an MOI of 1. At 3 dpi, cells were treated with 20 μM MG132 for 24 h prior to fixing onto glass slides (A) or for 6 h before washing three times in PBS (B) and incubating in normal maintenance medium for an additional 18 h before processing. ORF29p, ORF62p, and gE were detected by indirect immunofluorescence microscopy after incubation with specific antisera.

events or independent activities has not been established. We have previously shown that nuclear import of ORF29p occurs independent of the presence of other VZV-specified proteins via the classical nuclear import pathway, which is well conserved in most human cells (62). This was not surprising, as ORF29p enters the nuclei of infected neurons during reactivation. Nevertheless, the question of how ORF29p is excluded from the nucleus during latency remains.

In this report we demonstrate that differential compartmentalization of ORF29p is cell type dependent but can be altered in response to the expression of other virus proteins. Autonomous expression of ORF29p in U373MG cells and cultured guinea pig EG results in accumulation of this protein in the cytoplasm. This observation implies that nuclear exclusion during latency occurs independently of the distribution of other virus proteins. Because U373MG cells cannot support latent infection, we infer that the distribution profile of ORF29p is susceptible to change in response to expression of other VZV gene products. Specifically, we demonstrate that subsequent expression of either ORF61p or HSV-1 ICP0 results in the accumulation of ORF29p in the nuclei of cells where it normally remains cytoplasmic when autonomously expressed. This redistribution requires the protein's NLS, which is consistent with the hypothesis that the mechanism of ORF29p nuclear import is conserved among all human cell lines tested. The expression of ORF61p or ICP0 must, therefore, alter the environment of the host cell to permit redistribution to the nucleus. It is possible that during VZV latency a similar alteration in the pathogen-host interface induces reactivation.

The sensitivity of ORF29p subcellular localization to proteasome inhibitors revealed a role for the proteasome degradation system in this process. Proteasomes are large, multisubunit complexes, present in the nucleus and cytosol, that selectively degrade intracellular proteins. The pathway plays a major role in the degradation of many proteins involved in the cell cycle, proliferation, and apoptosis. The proteasome machinery also serves to remove abnormal proteins that might otherwise disrupt normal cellular homeostasis. A protein destined for degradation is generally marked by the covalent attachment of multiple ubiquitin moieties that escort it to the 26S proteasome for rapid hydrolysis. Ubiquitin is ligated to target proteins by a multienzymatic system consisting of ubiquitin-activating (E1), ubiquitin-conjugating (E2), and ubiquitin-ligating (E3) enzymes (32). An increase in the half-life of ORF29p in U373MG cells correlates with the nuclear accumulation of this protein following treatment with MG132, further implicating this pathway in the fate of ORF29p.

The short half-life of ORF29p in U373MG cells suggests that it is being directly targeted for degradation by the 26S proteasome. Additionally, at the 6-h time point during pulse-chase analysis in MeWo cells, antigenically related species that are both larger and smaller than ORF29p are detected, and they are less abundant in the samples treated with MG132 (Fig. 9A). ORF29p-related species with the same molecular weights are detected at all chase time points in U373MG cells and are also more abundant at later times in untreated cells (Fig. 9B). These larger and smaller ORF29p-related species that are also detected by Western analysis might represent modified and degraded peptides, respectively. The existence of similar species in both cell types suggests that the modification and breakdown of ORF29p occur ubiquitously but to various degrees. During productive VZV infection, ORF29p is detected at low levels in the cytoplasm of all cells (39, 49). Curiously, despite its presence in the cytoplasm, ORF29p is not packaged in the VZ virion, indicating that it does not gain access to the assembly machinery in the *trans*-Golgi network

(38, 60, 69). We speculate that the susceptibility of cytoplasmic ORF29p to degradation precludes it from being packaged.

During HSV-1 infection, ICP0 hijacks the ubiquitin-mediated proteasome degradation pathway components to create a cellular environment more conducive for productive infection. The interaction of ICP0 with the proteasome is normally dynamic, but in cells where the activity of the proteasome is inhibited, this association is stabilized (17, 22, 65). Our studies show that expression of ICP0 or ORF61p or inhibition of the proteasome results in nuclear localization of ORF29p. Mutations in regions of ICP0 involved in its association with components of the proteasome pathway abrogate its effect on ORF29p. We propose that this link between physical association and function results in sequestration by ICP0 of the proteasome machinery, with the result being stabilization of ORF29p. While there is no evidence for ORF61p involvement in the proteasome pathway, the most highly conserved domain between it and ICP0 is the ring finger encoded by exon 2. This domain has been demonstrated to possess E3 ubiquitin ligase activity and to bind the cdc32 E2 ubiquitin-conjugating enzyme (5, 17, 28, 65).

The enhanced stability of ORF29p correlates with its nuclear accumulation. Reversal of the action of MG132 demonstrates that ORF29p nuclear translocation does not guarantee its survival, as the protein's distribution and stability are reset when inhibition of proteasome activity is reversed. The stabilization of ORF29p, therefore, leads to its nuclear accumulation. The disappearance of ORF29p from the nucleus upon removal of the drug also suggests that ORF29p is either exported from or degraded in the nuclei of U373MG cells.

It was intriguing that although MG132 treatment induced ORF29p nuclear accumulation, this was not sufficient to reactivate latent VZV in cultured enteric neurons. Even after removal of MG132, virus remains latent and ORF29p reappears in the cytoplasm. Similar drug reversal experiments with U373MG cells in the presence of cycloheximide demonstrate that following reversal of inhibition of the proteasome, ORF29p is either destroyed in situ or exported for degradation. The regulation of ORF29p by the host cell during latency may therefore involve both nuclear exclusion and protein stability. MG132 treatment of latently infected neurons had no effect on ORF62p distribution, which suggests that compartmentalization of these two proteins during latency occurs via independent mechanisms. It is possible that a threshold for nuclear transport exists, as stabilization of the protein also allows for some nuclear accumulation.

The VZV infectious cycle is cell type specific in that invasion of the epidermis and dermis results in a lytic infection, while infection of the sensory ganglia leads to latency. ORF29p subcellular distribution and stability are also cell type dependent according to the state of VZV infection. Therefore, host factors must provide a cellular environment that is permissive to VZV latent infection. Our studies implicate the proteasome degradation pathway in control of the subcellular distribution of ORF29p. The involvement of the proteasome in cell-type-specific regulation of herpesvirus proteins has been documented for HSV-1 UL9, the virus DNA replication initiator, which is specifically targeted to the 26S proteasome in neurons (18, 19, 45). We postulate that fibroblasts may encode a mechanism that protects ORF29p from destruction and allows for nuclear import. Alternatively, U373MG cells and enteric neurons actively target ORF29p to the proteasome and thus abrogate nuclear translocation of this protein during AdORF29 infection.

In the context of VZV infection, it is conceivable that other virus-specified proteins also contribute to the mechanisms affecting ORF29p expression and subcellular distribution. The elucidation of the interplay between cellular pathways and virus proteins in the regulation of the differential compartmentalization of ORF29p and the other LAPs may expand our understanding of VZV latency and reactivation.

ACKNOWLEDGMENT

These studies were supported by Public Health Service grant AI-024021 to S.J.S.

REFERENCES

1. **Arvin, A. M.** 1996. Varicella-zoster virus. Clin. Microbiol. Rev. **9:**361–381.
2. **Assouline, J. G., M. J. Levin, E. O. Major, B. Forghani, S. E. Straus, and J. M. Ostrove.** 1990. Varicella-zoster virus infection of human astrocytes, Schwann cells, and neurons. Virology **179:**834–844.
3. **Boucaud, D., H. Yoshitake, J. Hay, and W. Ruyechan.** 1998. The varicella-zoster virus (VZV) open-reading frame 29 protein acts as a modulator of a late VZV gene promoter. J Infect. Dis. **178**(Suppl. 1)**:**S34–S38.
4. **Boutell, C., A. Orr, and R. D. Everett.** 2003. PML residue lysine 160 is required for the degradation of PML induced by herpes simplex virus type 1 regulatory protein ICP0. J. Virol. **77:**8686–8694.
5. **Boutell, C., S. Sadis, and R. D. Everett.** 2002. Herpes simplex virus type 1 immediate-early protein ICP0 and its isolated RING finger domain act as ubiquitin E3 ligases in vitro. J. Virol. **76:**841–850.
6. **Burch, A. D., and S. K. Weller.** 2004. Nuclear sequestration of cellular chaperone and proteasomal machinery during herpes simplex virus type 1 infection. J. Virol. **78:**7175–7185.
7. **Burkham, J., D. M. Coen, C. B. Hwang, and S. K. Weller.** 2001. Interactions of herpes simplex virus type 1 with ND10 and recruitment of PML to replication compartments. J. Virol. **75:**2353–2367.
8. **Chen, J., and S. Silverstein.** 1992. Herpes simplex viruses with mutations in the gene encoding ICP0 are defective in gene expression. J. Virol. **66:**2916–2927.
9. **Chen, J. J., A. A. Gershon, Z. S. Li, O. Lungu, and M. D. Gershon.** 2003. Latent and lytic infection of isolated guinea pig enteric ganglia by varicella zoster virus. J. Med. Virol. **70**(Suppl. 1)**:**S71–S8.
10. **Cohrs, R. J., M. Barbour, and D. H. Gilden.** 1996. Varicella-zoster virus (VZV) transcription during latency in human ganglia: detection of transcripts mapping to genes 21, 29, 62, and 63 in a cDNA library enriched for VZV RNA. J. Virol. **70:**2789–2796.
11. **Cohrs, R. J., M. B. Barbour, R. Mahalingam, M. Wellish, and D. H. Gilden.** 1995. Varicella-zoster virus (VZV) transcription during latency in human ganglia: prevalence of VZV gene 21 transcripts in latently infected human ganglia. J. Virol. **69:**2674–2678.
12. **Cohrs, R. J., D. H. Gilden, P. R. Kinchington, E. Grinfeld, and P. G. Kennedy.** 2003. Varicella-zoster virus gene 66 transcription and translation in latently infected human ganglia. J. Virol. **77:**6660–6665.
13. **Cohrs, R. J., K. Srock, M. B. Barbour, G. Owens, R. Mahalingam, M. E. Devlin, M. Wellish, and D. H. Gilden.** 1994. Varicella-zoster virus (VZV) transcription during latency in human ganglia: construction of a cDNA library from latently infected human trigeminal ganglia and detection of a VZV transcript. J. Virol. **68:**7900–7908.
14. **Cohrs, R. J., J. Wischer, C. Essman, and D. H. Gilden.** 2002. Characterization of varicella-zoster virus gene 21 and 29 proteins in infected cells. J. Virol. **76:**7228–7238.
15. **Croen, K. D., J. M. Ostrove, L. J. Dragovic, and S. E. Straus.** 1988. Patterns of gene expression and sites of latency in human nerve ganglia are different for varicella-zoster and herpes simplex viruses. Proc. Natl. Acad. Sci. USA **85:**9773–9777.
16. **Croen, K. D., and S. E. Straus.** 1991. Varicella-zoster virus latency. Annu. Rev. Microbiol. **45:**265–282.
17. **Diao, L., B. Zhang, J. Fan, X. Gao, S. Sun, K. Yang, D. Xin, N. Jin, Y. Geng, and C. Wang.** 2005. Herpes virus proteins ICP0 and BICP0 can activate NF-kappaB by catalyzing IkappaBalpha ubiquitination. Cell Signal. **17:**217–229.
18. **Eom, C. Y., W. D. Heo, M. L. Craske, T. Meyer, and I. R. Lehman.** 2004. The neural F-box protein NFB42 mediates the nuclear export of the herpes simplex virus type 1 replication initiator protein (UL9 protein) after viral infection. Proc. Natl. Acad. Sci. USA **101:**4036–4040.
19. **Eom, C. Y., and I. R. Lehman.** 2003. Replication-initiator protein (UL9) of the herpes simplex virus 1 binds NFB42 and is degraded via the ubiquitin-proteasome pathway. Proc. Natl. Acad. Sci. USA **100:**9803–9807.

20. **Everett, R. D.** 2000. ICP0, a regulator of herpes simplex virus during lytic and latent infection. Bioessays **22:**761–770.
21. **Everett, R. D.** 1986. The products of herpes simplex virus type 1 (HSV-1) immediate early genes 1, 2 and 3 can activate HSV-1 gene expression in trans. J. Gen. Virol. **67:**2507–2513.
22. **Everett, R. D., A. Orr, and C. M. Preston.** 1998. A viral activator of gene expression functions via the ubiquitin-proteasome pathway. EMBO J. **17:** 7161–7169.
23. **Gelman, I. H., and S. Silverstein.** 1986. Co-ordinate regulation of herpes simplex virus gene expression is mediated by the functional interaction of two immediate early gene products. J. Mol. Biol. **191:**395–409.
24. **Graham, F. L., J. Smiley, W. C. Russell, and R. Nairn.** 1977. Characteristics of a human cell line transformed by DNA from human adenovirus type 5. J. Gen. Virol. **36:**59–74.
25. **Grinfeld, E., and P. G. Kennedy.** 2004. Translation of varicella-zoster virus genes during human ganglionic latency. Virus Genes **29:**317–319.
26. **Grose, C., and P. A. Brunel.** 1978. Varicella-zoster virus: isolation and propagation in human melanoma cells at 36 and 32 degrees C. Infect. Immun. **19:**199–203.
27. **Gu, H., Y. Liang, G. Mandel, and B. Roizman.** 2005. Components of the REST/CoREST/histone deacetylase repressor complex are disrupted, modified, and translocated in HSV-1-infected cells. Proc. Natl. Acad. Sci. USA **102:**7571–7576.
28. **Hagglund, R., C. Van Sant, P. Lopez, and B. Roizman.** 2002. Herpes simplex virus 1-infected cell protein 0 contains two E3 ubiquitin ligase sites specific for different E2 ubiquitin-conjugating enzymes. Proc. Natl. Acad. Sci. USA **99:**631–636.
29. **Hamamoto, T., S. Gunji, H. Tsuji, and T. Beppu.** 1983. Leptomycins A and B, new antifungal antibiotics. I. Taxonomy of the producing strain and their fermentation, purification and characterization. J. Antibiot. (Tokyo) **36:**639–645.
30. **Harris, R. A., R. D. Everett, X. X. Zhu, S. Silverstein, and C. M. Preston.** 1989. Herpes simplex virus type 1 immediate-early protein Vmw110 reactivates latent herpes simplex virus type 2 in an in vitro latency system. J. Virol. **63:**3513–3515.
31. **Hay, J., and W. T. Ruyechan.** 1994. Varicella-zoster virus: a different kind of herpesvirus latency? Semin. Virol. **5:**241–248.
32. **Hershko, A., and A. Ciechanover.** 1998. The ubiquitin system. Annu. Rev. Biochem. **67:**425–479.
33. **Inchauspe, G., S. Nagpal, and J. M. Ostrove.** 1989. Mapping of two varicella-zoster virus-encoded genes that activate the expression of viral early and late genes. Virology **173:**700–709.
34. **Jordan, R., and P. A. Schaffer.** 1997. Activation of gene expression by herpes simplex virus type 1 ICP0 occurs at the level of mRNA synthesis. J. Virol. **71:**6850–6862.
35. **Kamei, Y., S. Yuba, T. Nakayama, and Y. Yoneda.** 1999. Three distinct classes of the alpha-subunit of the nuclear pore-targeting complex (importin-alpha) are differentially expressed in adult mouse tissues. J. Histochem Cytochem. **47:**363–372.
36. **Kennedy, P. G., E. Grinfeld, and J. E. Bell.** 2000. Varicella-zoster virus gene expression in latently infected and explanted human ganglia. J. Virol. **74:** 11893–11898.
37. **Kennedy, P. G., E. O. Major, R. K. Williams, and S. E. Straus.** 1994. Down-regulation of glial fibrillary acidic protein expression during acute lytic varicella-zoster virus infection of cultured human astrocytes. Virology **205:** 558–562.
38. **Kinchington, P. R., D. Bookey, and S. E. Turse.** 1995. The transcriptional regulatory proteins encoded by varicella-zoster virus open reading frames (ORFs) 4 and 63, but not ORF 61, are associated with purified virus particles. J. Virol. **69:**4274–4282.
39. **Kinchington, P. R., G. Inchauspe, J. H. Subak-Sharpe, F. Robey, J. Hay, and W. T. Ruyechan.** 1988. Identification and characterization of a varicella-zoster virus DNA-binding protein by using antisera directed against a predicted synthetic oligopeptide. J. Virol. **62:**802–809.
40. **Kinchington, P. R., and S. E. Turse.** 1998. Regulated nuclear localization of the varicella-zoster virus major regulatory protein, IE62. J. Infect. Dis. **178**(Suppl. 1)**:**S16–S21.
41. **Kisselev, A. F., and A. L. Goldberg.** 2001. Proteasome inhibitors: from research tools to drug candidates. Chem. Biol. **8:**739–758.
42. **Kohler, M., C. Speck, M. Christiansen, F. R. Bischoff, S. Prehn, H. Haller, D. Gorlich, and E. Hartmann.** 1999. Evidence for distinct substrate specificities of importin alpha family members in nuclear protein import. Mol. Cell. Biol. **19:**7782–7791.
43. **Kudo, N., B. Wolff, T. Sekimoto, E. P. Schreiner, Y. Yoneda, M. Yanagida, S. Horinouchi, and M. Yoshida.** 1998. Leptomycin B inhibition of signal-mediated nuclear export by direct binding to CRM1. Exp. Cell Res. **242:**540–547.
44. **Lee, D. H., and A. L. Goldberg.** 1998. Proteasome inhibitors: valuable new tools for cell biologists. Trends Cell Biol. **8:**397–403.
45. **Lee, S. S., and I. R. Lehman.** 1997. Unwinding of the box I element of a herpes simplex virus type 1 origin by a complex of the viral origin binding protein, single-strand DNA binding protein, and single-stranded DNA. Proc. Natl. Acad. Sci. USA **94:**2838–2842.
46. **Lees-Miller, S. P., M. C. Long, M. A. Kilvert, V. Lam, S. A. Rice, and C. A. Spencer.** 1996. Attenuation of DNA-dependent protein kinase activity and its catalytic subunit by the herpes simplex virus type 1 transactivator ICP0. J. Virol. **70:**7471–7477.
47. **Li, M., C. L. Brooks, F. Wu-Baer, D. Chen, R. Baer, and W. Gu.** 2003. Mono- versus polyubiquitination: differential control of p53 fate by Mdm2. Science **302:**1972–1975.
48. **Lomonte, P., J. Thomas, P. Texier, C. Caron, S. Khochbin, and A. L. Epstein.** 2004. Functional interaction between class II histone deacetylases and ICP0 of herpes simplex virus type 1. J. Virol. **78:**6744–6757.
49. **Lungu, O., C. A. Panagiotidis, P. W. Annunziato, A. A. Gershon, and S. J. Silverstein.** 1998. Aberrant intracellular localization of Varicella-Zoster virus regulatory proteins during latency. Proc. Natl. Acad. Sci. USA **95:**7080–7085.
50. **Meier, J. L., R. P. Holman, K. D. Croen, J. E. Smialek, and S. E. Straus.** 1993. Varicella-zoster virus transcription in human trigeminal ganglia. Virology **193:**193–200.
51. **Meier, J. L., X. Luo, M. Sawadogo, and S. E. Straus.** 1994. The cellular transcription factor USF cooperates with varicella-zoster virus immediate-early protein 62 to symmetrically activate a bidirectional viral promoter. Mol. Cell. Biol. **14:**6896–6906.
52. **Meier, J. L., and S. E. Straus.** 1995. Interactions between varicella-zoster virus IE62 and cellular transcription factor USF in the coordinate activation of genes 28 and 29. Neurology **45:**S30–S32.
53. **Meier, J. L., and S. E. Straus.** 1993. Varicella-zoster virus DNA polymerase and major DNA-binding protein genes have overlapping divergent promoters. J. Virol. **67:**7573–7581.
54. **Ng, P., D. T. Cummings, C. M. Evelegh, and F. L. Graham.** 2000. Yeast recombinase FLP functions effectively in human cells for construction of adenovirus vectors. BioTechniques **29:**524–526, 528.
55. **O'Hare, P., and G. S. Hayward.** 1985. Evidence for a direct role for both the 175,000- and 110,000-molecular-weight immediate-early proteins of herpes simplex virus in the transactivation of delayed-early promoters. J. Virol. **53:**751–760.
56. **O'Hare, P., and G. S. Hayward.** 1985. Three trans-acting regulatory proteins of herpes simplex virus modulate immediate-early gene expression in a pathway involving positive and negative feedback regulation. J. Virol. **56:**723–733.
57. **Parkinson, J., S. P. Lees-Miller, and R. D. Everett.** 1999. Herpes simplex virus type 1 immediate-early protein vmw110 induces the proteasome-dependent degradation of the catalytic subunit of DNA-dependent protein kinase. J. Virol. **73:**650–657.
58. **Philipson, L.** 1961. Adenovirus assay by the fluorescent cell-counting procedure. Virology **15:**263–268.
59. **Poon, A. P., S. J. Silverstein, and B. Roizman.** 2002. An early regulatory function required in a cell type-dependent manner is expressed by the genomic but not the cDNA copy of the herpes simplex virus 1 gene encoding infected cell protein 0. J. Virol. **76:**9744–9755.
60. **Roberts, C. R., A. C. Weir, J. Hay, S. E. Straus, and W. T. Ruyechan.** 1985. DNA-binding proteins present in varicella-zoster virus-infected cells. J. Virol. **55:**45–53.
61. **Rost, B., and J. Liu.** 2003. The PredictProtein server. Nucleic Acids Res. **31:**3300–3304.
62. **Stallings, C. L., and S. Silverstein.** 2005. Dissection of a novel nuclear localization signal in open reading frame 29 of varicella-zoster virus. J. Virol. **79:**13070–13081.
63. **Straus, S. E.** 1993. Shingles. Sorrows, salves, and solutions. JAMA **269:**1836–1839.
64. **Taylor, T. J., and D. M. Knipe.** 2003. C-terminal region of herpes simplex virus ICP8 protein needed for intranuclear localization. Virology **309:**219–231.
65. **Van Sant, C., R. Hagglund, P. Lopez, and B. Roizman.** 2001. The infected cell protein 0 of herpes simplex virus 1 dynamically interacts with proteasomes, binds and activates the cdc34 E2 ubiquitin-conjugating enzyme, and possesses in vitro E3 ubiquitin ligase activity. Proc. Natl. Acad. Sci. USA **98:**8815–8820.
66. **Yang, M., J. Hay, and W. T. Ruyechan.** 2004. The DNA element controlling expression of the varicella-zoster virus open reading frame 28 and 29 genes consists of two divergent unidirectional promoters which have a common USF site. J. Virol. **78:**10939–10952.
67. **Zhu, X. X., J. X. Chen, C. S. Young, and S. Silverstein.** 1990. Reactivation of latent herpes simplex virus by adenovirus recombinants encoding mutant IE-0 gene products. J. Virol. **64:**4489–4498.
68. **Zhu, X. X., C. S. Young, and S. Silverstein.** 1988. Adenovirus vector expressing functional herpes simplex virus ICP0. J. Virol. **62:**4544–4553.
69. **Zhu, Z., M. D. Gershon, Y. Hao, R. T. Ambron, C. A. Gabel, and A. A. Gershon.** 1995. Envelopment of varicella-zoster virus: targeting of viral glycoproteins to the trans-Golgi network. J. Virol. **69:**7951–7959.